Monthly Notices of the ROYAL ASTRONOMICAL SOCIETY

Mon. Not. R. Astron. Soc. **425,** 3002–3023 (2012) doi:10.1111/j.1365-2966.2012.21583.x

Optical flux and spectral variability of blazars

Haritma Gaur,[1,2]★ Alok C. Gupta,[1,2] A. Strigachev,[3] R. Bachev,[3] E. Semkov,[3] Paul J. Wiita,[4] S. Peneva,[3] S. Boeva,[3] L. Slavcheva-Mihova,[3] B. Mihov,[3] G. Latev[3] and U. S. Pandey[2]

[1]*Aryabhatta Research Institute of Observational Sciences (ARIES), Manora Peak, Nainital 263129, India*
[2]*Department of Physics, DDU Gorakhpur University, Gorakhpur 273009, India*
[3]*Institute of Astronomy and National Astronomical Observatory, Bulgarian Academy of Sciences, 72 Tsarigradsko Shosse Blvd., 1784 Sofia, Bulgaria*
[4]*Department of Physics, The College of New Jersey, PO Box 7718, Ewing, NJ 08628-0718, USA*

Accepted 2012 June 24. Received 2012 June 8; in original form 2012 February 1

ABSTRACT

We report the results of optical monitoring for a sample of 11 blazars including 10 BL Lacertae objects (BL Lacs) and one flat spectrum radio quasar (FSRQ). We have measured the multiband optical flux and colour variations in these blazars on intraday and short-term time-scales of months and have limited data for two more blazars. These photometric observations were made during 2009–2011, using six optical telescopes, four in Bulgaria, one in Greece and one in India. On short-term time-scales we found significant flux variations in nine of the sources and colour variations in three of them. Intraday variability was detected on six nights for two sources out of the 18 nights and four sources for which we collected such data. These new optical observations of these blazars plus data from our previous published papers (for three more blazars) were used to analyse their spectral flux distributions in the optical frequency range. Our full sample for this purpose includes six high-synchrotron-frequency-peaked BL Lacs (HSPs), three intermediate-synchrotron-frequency-peaked BL Lacs (ISPs) and six low-synchrotron-frequency-peaked BL Lacs (LSPs; including both BL Lacs and FSRQs). We also investigated the spectral slope variability and found that the average spectral slopes of LSPs show a good accordance with the synchrotron self-Compton loss dominated model. Our analysis supports previous studies that found that the spectra of the HSPs and FSRQs have significant additional emission components. The spectra of all these HSPs and LSPs get flatter when they become brighter, while for FSRQs the opposite appears to hold. This supports the hypothesis that there is a significant thermal contribution to the optical spectrum for FSRQs.

Key words: galaxies: active – BL Lacertae objects: general – galaxies: jets – galaxies: photometry.

1 INTRODUCTION

Blazars are a very active class of active galactic nuclei (AGN), consisting of optically violently variable quasars, flat spectrum radio quasars (FSRQs) and BL Lacertae objects (BL Lacs). In some cases, their emission lines are very weak or absent (equivalent width <5 Å), a property which classically was used to define the BL Lacs (Stocke et al. 1991; Marcha et al. 1996). Other blazars have broad emission lines similar to those of normal quasars. They have been observed at all wavelengths, from radio through very high energy (VHE) γ-rays. Blazars exhibit variability at all wavelengths on various time-scales. The high inferred isotropic luminosities and apparent superluminal motion revealed by long baseline radio interferometry provide conclusive evidence that blazars are sources with relativistic jets oriented close to our line of sight and their emission is highly beamed and Doppler boosted in the forward direction.

The overall emission from radio to γ-rays shows the presence of two well-defined broad components (von Montigny et al. 1995; Fossati et al. 1998). The dominant emission mechanisms in all classes of blazars is most likely synchrotron emission from radio to UV/soft X-ray frequencies and inverse Compton scattering for hard X-ray and γ-ray energies. The spectral energy distribution (SED) of low synchrotron frequency peaked BL Lacs (LSPs) and high synchrotron frequency peaked BL Lacs (HSPs) are systematically different, with the observed peak of the emitted power typically at near-infrared (NIR)/optical wavelengths for LSPs and at ultraviolet (UV)/soft X-ray wavelengths for HSPs (Giommi, Ansari & Micol

★E-mail: haritma@aries.res.in

1995). One can define the objects as LSPs or HSPs if their ratio of X-ray flux in the 0.3–3.5 keV band to radio flux density at 5 GHz is smaller than or larger than $10^{-11.5}$, respectively (Padovani & Giommi 1996). However, SED peaks can be located at intermediate frequencies as well, giving rise to the intermediate synchrotron peaked blazar (ISP) classification (Sambruna, Maraschi & Urry 1996). Nieppola, Tornikoski & Valtaoja (2006) classify over 300 BL Lacs and suggest that blazars with energy peak frequency, $\nu_{\rm peak} \sim 10^{13-14}$ Hz are LSPs, those with $\nu_{\rm peak} \sim 10^{15-16}$ Hz are ISPs and those with $\nu_{\rm peak} \sim 10^{17-18}$ Hz are HSPs. Recently, Abdo et al. (2010) extended the definition to all types of non-thermal-dominated AGN depending on the peak frequency of their synchrotron hump, $\nu_{\rm peak}$, and suggest the following classification: LSP sources with $\nu_{\rm peak} \leq 10^{14}$ Hz; ISP sources with $10^{14} < \nu_{\rm peak} < 10^{15}$ Hz and HSP sources with $\nu_{\rm peak} \geq 10^{15}$ Hz; however, we have used the broader definition of ISPs put forward by Nieppola et al. (2006).

Optical observations offer a wealth of information on the variability of blazars and play an important role in discriminating between LSPs and HSPs. Differences in the optical spectral properties of LSPs and HSPs constrain the theoretical models that try to explain the spectra and variability of these blazars.

The study of SED properties is an excellent diagnostic tool for theoretical models and for the understanding of the physical radiation mechanisms, as these studies are crucial in analysing individual emission components. With respect to the optical spectrum of blazars, for HSPs, the maximum is located at higher frequencies and so the optical emission is in the ascending part of the synchrotron emission hump, while for LSPs the optical emission is expected to be in the descending part of this portion of the SED. Thus we expect for HSPs that the radio-through-X-ray spectral index $\alpha_{\rm RX}$ is less than or equal to 0.75 or 0.80, while for LSPs, it is greater than 0.75 (Urry & Padovani 1995) or 0.80, whereas for ISPs, $0.7 \leq \alpha_{\rm RX} \leq 0.8$ (Sambruna et al. 1996).

Although the optical band is very narrow with respect to other spectral bands, it may yield a large amount of information, as it can indicate the possible presence of other components in addition to the synchrotron continuum. For example, thermal emission from the accretion disc around the central engine is an important physical component, while the emission from the surrounding region of the nucleus and the host galaxy contribution are fundamentally contaminants. The synchrotron inverse-Compton emission model predicts that the spectrum gets harder as the source turns brighter and several investigators indeed found that the optical spectrum became flatter when the flux increased, while the spectrum became steeper when the flux decreased (e.g. Gear, Robson & Brown 1986; Maesano et al. 1997). However, Ghosh et al. (2000) suggested that this might not be always correct. Trèvese & Vagnetti (2002) analysed the spectral slope variability of 42 PG quasars and concluded that the spectral variability must be intrinsic to the nuclear component. Vagnetti, Trèvese & Nesci (2003) showed that the spectral variability, even restricted to the optical band, could be used to set limits on the relative contribution of the synchrotron component and the thermal component.

Here we report the optical observations of 11 blazars on intraday variability (IDV) and short-term variability (STV; from days through months) time-scales during the 2009–2011 observing seasons. We also searched for colour variations in these blazars on intraday and short-term time-scales. In addition, we analysed the main features of the optical spectra for our sample of blazars.

The paper is structured as follows. In Section 2, we present the observations and data reduction procedure, including our approaches to variability and time-scale detection. Section 3 provides our results of IDV, STV and colour variability of our sample of blazars. Section 4 gives the general characteristics of the optical spectra. Section 5 provides the results of flux, colour and spectral variability of these sources, and we have presented our conclusions in Section 6.

Table 1. Details of telescope and instrument.

Site	NAO, Rozhen
Telescope	60-cm Cassegrain
CCD model	FLI Pl09000
Chip size	3056×3056 pixels
Pixel size	12×12 μm
Scale[a]	0.330 arcsec pixel^{-1}
Field	16.8×16.8 arcmin^2
Gain	1.0 e$^-$ ADU^{-1}
Read out noise	8.5 e$^-$ rms
Binning used	2×2
Typical seeing	1.5–3.5 arcsec

[a]With a binning factor of 1×1.

2 OBSERVATIONS AND DATA REDUCTION

Observations of these blazars were performed using six optical telescopes, four in Bulgaria, one in Greece and one in India. All of these telescopes are equipped with CCD detectors and Johnson *UBV* and Cousins *RI* filters. Details of five of these telescopes, detectors and other parameters related to the observations are given in table 1 of Gaur et al. (2012b) and a description of the remaining telescope is given in Table 1. A complete log of observations of these blazars from those six telescopes is given in Table 2. Although we have observed 13 blazars as part of this study, for our analyses of STV and colour variations, we used only 11 blazars, since the blazars J0211+1051 and 1ES 0806+524 were each only observed on four nights.

We carried out optical photometric observations during the period 2009–2011. The raw photometric data were processed by standard methods. Image processing or pre-processing was done using standard routines in the Image Reduction and Analysis Facility[1] (IRAF) and ESO-MIDAS[2] softwares.

We processed the data using the Dominion Astrophysical Observatory Photometry (DAOPHOT II) software to perform the circular concentric aperture photometric technique (Stetson 1987, 1992). For each night we carried out aperture photometry with four different aperture radii, i.e. 1 × full width at half-maximum (FWHM), 2 × FWHM, 3 × FWHM and 4 × FWHM. On comparing the photometric results we found that aperture radii of 2 × FWHM almost always provided the best signal-to-noise (S/N) ratio, so we adopted that aperture for our final results.

For these blazars, we observed three or more local standard stars on the same fields. We employed two standard stars from each blazar field with magnitudes similar to those of the target and plotted their differential instrumental magnitudes for the IDV light curves. As the fluxes of the blazars and the standard stars were obtained simultaneously and so at the same air mass and with identical instrumental

[1] IRAF is distributed by the National Optical Astronomy Observatories, which are operated by the Association of Universities for Research in Astronomy, Inc., under cooperative agreement with the National Science Foundation.
[2] ESO-MIDAS is the acronym for the European Southern Observatory Munich Image Data Analysis System which is developed and maintained by European Southern Observatory.

Table 2. Observation log of optical photometric observations.

Source (z)	$\alpha_{2000.0}$ (hh mm ss)	$\delta_{2000.0}$ (hh mm ss)	Date of observation (yyyy mm dd)	Telescope	Data points (B,V,R,I)
3C 66A	02 22 39.61	+43 02 07.80	2009 11 13	D	2,2,2,2
(0.444)			2009 11 14	D	2,2,2,2
			2009 11 18	C	1,2,2,2
			2009 11 19	C	2,2,2,2
			2009 11 20	C	2,2,2,3
			2009 11 21	C	2,2,2,2
			2009 11 22	C	5,2,2,2
			2009 11 23	C	4,2,2,4
			2009 11 24	C	3,3,2,2
			2009 11 25	B	2,3,2,2
			2009 12 21	B	2,2,3,2
			2010 11 01	C	2,2,2,2
			2010 11 03	D	0,4,4,4
			2010 11 04	D	0,2,2,2
			2010 11 05	D	3,2,2,2
			2010 11 06	D	4,4,4,4
J0211+1051	02 11 03.20	+10 51 32.00	2011 01 25	D	0,3,3,3
(0.20)			2011 01 26	D	3,3,3,3
			2011 01 27	D	2,2,2,2
			2011 02 07	C	2,2,2,2
AO 0235+164	02 38 39.93	+16 36 59.27	2009 11 13	D	2,2,2,2
(0.94)			2009 11 14	D	2,2,2,2
			2009 11 18	C	0,0,1,1
			2009 11 19	C	0,0,2,3
			2009 11 20	C	0,0,2,2
			2009 11 21	C	0,0,2,2
			2009 11 25	B	2,3,2,3
			2010 11 06	D	0,0,1,1
S5 0716+714	07 21 53.45	+71 20 36.35	2009 11 14	D	2,2,2,2
(0.31 ± 0.08)			2009 11 15	C	2,2,2,2
			2009 11 16	C	2,2,2,2
			2009 11 19	C	2,2,2,2
			2009 11 21	C	2,2,2,2
			2009 11 22	C	2,2,2,2
			2009 11 26	B	2,2,2,2
			2009 12 11	A	0,0,61,0
			2009 12 13	A	1,1,105,1
			2009 12 15	A	1,1,115,1
			2009 12 21	B	3,3,3,3
			2010 01 11	C	2,2,2,2
			2010 02 03	C	2,2,2,2
			2010 11 02	C	2,2,2,2
			2011 01 02	C	2,2,2,2
			2011 02 03	C	3,2,2,3
			2011 03 04	C	2,2,2,2
			2011 03 24	C	2,3,3,2
			2011 03 25	C	2,2,2,2
1ES 0806+524	08 09 49.19	+52 18 58.40	2011 01 25	D	2,2,2,2
(0.138)			2011 02 06	C	2,2,2,2
			2011 02 07	C	2,2,2,2
			2011 05 27	D	0,2,2,2
OJ 287	08 54 48.87	+20 06 30.64	2009 11 13	D	2,2,2,2
(0.306)			2009 11 15	C	2,2,2,2
			2009 11 20	C	2,2,2,2
			2009 11 21	C	2,2,2,2
			2009 11 21	A	1,1,1,1
			2009 11 22	A	1,1,35,1
			2009 11 22	C	2,2,2,2
			2009 11 26	B	2,2,2,2
			2009 12 21	A	1,1,132,1
			2010 01 10	A	1,1,90,1
			2010 01 11	A	1,1,80,1

Table 2 – *continued*

Source (z)	$\alpha_{2000.0}$ (hh mm ss)	$\delta_{2000.0}$ (hh mm ss)	Date of observation (yyyy mm dd)	Telescope	Data points (B,V,R,I)
			2010 01 11	C	2,2,2,2
			2010 01 20	A	1,1,95,1
			2010 02 03	C	3,3,3,3
			2010 03 16	E	3,3,3,3
			2010 11 02	C	2,2,2,2
Mrk 421	11 04 27.20	+38 12 32.00	2009 11 15	C	2,2,2,2
(0.031)			2009 11 21	C	2,2,2,2
			2009 11 22	C	2,2,2,2
			2009 11 26	B	2,2,2,2
			2010 01 11	C	2,2,2,2
			2010 02 03	C	2,2,2,2
			2010 03 06	D	2,2,2,2
			2010 03 16	E	2,2,2,2
			2010 04 03	C	2,2,2,2
			2010 05 14	C	2,2,2,2
			2010 06 07	C	2,2,2,2
			2010 06 10	C	2,2,2,2
			2010 06 12	C	2,2,2,2
			2011 01 02	C	2,2,2,2
			2011 02 05	D	2,2,2,2
			2011 02 08	D	2,2,2,2
			2011 05 02	D	2,2,2,2
1ES 1218+304	12 21 21.94	+30 10 37.11	2011 05 02	D	0,2,2,2
(0.182)			2011 05 27	D	0,2,2,2
			2011 05 29	D	0,2,2,2
			2011 06 23	D	0,2,2,2
			2011 06 26	D	0,2,2,2
			2011 07 06	C	2,2,2,2
ON 231	12 21 31.69	+28 13 58.50	2009 11 15	C	2,2,2,2
(0.102)			2009 11 21	C	2,2,2,2
			2009 11 22	C	2,2,2,2
			2009 11 26	B	2,2,2,2
			2010 01 11	Bfr	2,3,2,4
			2010 02 03	C	2,2,2,2
			2010 03 06	D	2,2,2,2
			2010 03 16	E	2,2,2,2
			2010 04 04	C	2,2,2,2
			2010 05 13	C	2,2,2,2
			2010 05 14	C	2,2,2,2
			2010 06 07	C	2,2,2,2
			2010 06 08	C	2,2,2,2
			2010 06 10	C	2,2,2,2
			2010 06 12	C	2,2,2,2
			2010 08 06	C	2,2,2,2
			2011 02 06	C	2,2,2,2
3C 279	12 56 11.17	−05 47 21.52	2011 05 27	D	2,2,2,2
(0.5362)			2011 05 28	D	2,2,2,2
			2011 05 29	D	2,2,2,2
			2011 05 31	D	0,2,2,2
			2011 06 08	B	2,2,2,2
			2011 06 09	C	0,2,2,2
			2011 06 21	C	0,2,2,2
			2011 06 22	C	0,2,2,2
			2011 06 23	C	0,2,2,2
			2011 06 23	D	0,2,2,2
			2011 06 24	C	0,2,2,2
1ES 1426+428	14 28 36.60	+42 40 21.00	2010 03 16	E	3,3,3,3
(0.129)			2010 03 17	E	2,2,83,1
			2010 03 17	A	0,0,32,0
			2010 04 04	C	0,2,2,2
			2010 05 14	C	1,1,1,1
			2010 06 04	C	2,2,2,3

Table 2 – *continued*

Source (z)	$\alpha_{2000.0}$ (hh mm ss)	$\delta_{2000.0}$ (hh mm ss)	Date of observation (yyyy mm dd)	Telescope	Data points (B,V,R,I)
			2010 06 07	C	1,2,2,3
			2010 06 12	C	2,2,2,2
			2010 06 18	F	62,2,62,2
			2010 06 21	F	62,2,62,2
			2010 07 15	D	0,2,2,2
			2010 07 16	D	0,2,2,2
			2010 08 06	C	0,0,2,2
			2011 02 08	C	3,2,3,2
1ES 1553+113	15 55 43.04	+11 11 24.37	2010 03 18	E	3,3,3,3
(0.360)			2010 05 07	C	2,2,111,2
			2010 05 14	C	4,4,4,4
			2010 06 08	C	2,2,2,2
			2010 06 10	C	2,2,2,2
			2010 06 11	C	2,2,120,2
			2010 06 12	D	50,2,50,2
			2010 06 14	D	24,2,21,2
			2010 06 20	F	61,2,61,2
			2010 06 22	F	57,2,57,2
			2010 07 15	D	3,2,2,2
			2010 07 16	D	3,2,2,2
			2010 07 17	D	3,2,2,2
			2010 07 17	C	2,2,2,2
			2010 08 06	C	2,2,2,2
BL Lac	22 02 43.29	+42 16 39.98	2009 07 15	C	0,0,15,0
(0.069)			2010 06 12	C	2,2,2,2
			2010 06 13	C	2,2,2,2
			2010 06 14	D	3,2,2,2
			2010 06 15	D	4,3,3,3
			2010 06 17	D	5,5,5,3

Note. A: 1.04-m Sampuranand Telescope, ARIES, Nainital, India.
B: 2-m Ritchey-Chretien telescope at National Astronomical Observatory, Rozhen, Bulgaria.
Bfr: 2-m Ritchey-Chretien telescope with focal reducer (FoReRo2) at the National Astronomical Observatory, Rozhen, Bulgaria.
C: 50/70-cm Schmidt telescope at National Astronomical Observatory, Rozhen, Bulgaria.
D: 60-cm Cassegrain telescope at Astronomical Observatory, Belogradchik, Bulgaria.
E: 60-cm Cassegrain telescope at National Astronomical Observatory, Rozhen, Bulgaria.
F: 1.3-m Ritchey-Chretien telescope at Skinakas Observatory, University of Crete, Greece.

and weather conditions, the flux ratios are considered to be very reliable. Finally, to calibrate the photometry of the blazars, we used the one standard star that had a colour closer to that of the blazar.

2.1 Variability detection criterion

To search for and describe blazar variability we have employed two quantities commonly used in the literature.

2.1.1 C-test

The variability detection parameter, C, was introduced by Romero, Cellone & Combi (1999), and is defined as the average of $C1$ and $C2$ where

$$C1 = \frac{\sigma(\mathrm{BL}-\mathrm{starA})}{\sigma(\mathrm{starA}-\mathrm{starB})} \quad \text{and} \quad C2 = \frac{\sigma(\mathrm{BL}-\mathrm{starB})}{\sigma(\mathrm{starA}-\mathrm{starB})}. \tag{1}$$

Here, (BL–starA) and (BL–starB) are the differential instrumental magnitudes of the blazar and standard star A and the blazar and standard star B, respectively, while σ(BL–starA), σ(BL–starB) and σ(starA–starB) are the observational scatters of the differential instrumental magnitudes of the blazar and star A, the blazar and star B and starA and star B, respectively. If $C \geq 2.576$, the nominal confidence level of a variability detection is >99 per cent. However, this C-test is not a true statistic as it is not appropriately distributed and this criterion is usually too conservative (de Diego 2010).

2.1.2 F-test

We test our results for variability using the standard F-test, which is a properly distributed statistic (de Diego 2010). Given two sample variances such as s_Q^2 for the blazar instrumental light-curve measurements and s_*^2 for that of the standard star, then

$$F = \frac{s_Q^2}{s_*^2}. \tag{2}$$

The number of degrees of freedom for each sample, ν_Q and ν_*, will be the same and equal to the number of measurements, N, minus 1 ($\nu = N - 1$). The F value is then compared with the $F^{(\alpha)}_{\nu_Q,\nu_*}$ critical value, where α is the significance level set for the test. The smaller the α value, the more improbable that the result is produced by chance. If F is larger than the critical value, the null hypothesis (no variability) is discarded. We have performed F-tests

at two significance levels (0.1 and 1 per cent) which correspond to 3σ and 2.6σ detections, respectively.

2.2 Time-scale of variability detection methods

2.2.1 Structure function

The structure function (SF) is a useful tool to make preliminary estimates of any periodicities and time-scales in time series data and is able to discern the range of the characteristic time-scales that contribute to the fluctuations. For details about how we used the SF see Gaur et al. (2010). Emmanoulopoulos, McHardy & Uttley (2010) have discussed the weaknesses of the SF method, so we have cross-checked our SF results by the discrete correlation function (DCF) method.

2.2.2 Discrete correlation function

The DCF is analogous to the classical correlation function which requires evenly sampled data except that it can work with unevenly sampled data. It was introduced by Edelson & Krolik (1988). Hufnagel & Bregman (1992) generalized the method to include a better error estimate. For details about the DCF see Tornikoski et al. (1994), Hovatta et al. (2007) and references therein.

3 RESULTS

3.1 Intraday, short-term flux and colour variability of individual blazars

3.1.1 3C 66A

3C 66A was classified as a BL Lac object by Maccagni et al. (1987), based on its significant optical and X-ray variability with its redshift at $z = 0.444$ (Lanzetta, Turnshek & Sandoval 1993) that value is actually quite uncertain (e.g. Bramel et al. 2005). The synchrotron peak of this source is located between 10^{15} and 10^{16} (Perri et al. 2003) and therefore 3C 66A can be classified as an ISP. It shows highly variable non-thermal continuum emission ranging from radio up to X-ray and to γ-ray frequencies on different time-scales and exhibits strong polarization from radio to optical wavelengths (e.g. Maraschi et al. 1994; Urry & Padovani 1995; Hartman et al. 1999; Gupta et al. 2008; Bauer et al. 2009; Villata et al. 2009). Long-term optical variability and spectral variability have been studied before (Fan & Lin 2000; Vagnetti et al. 2003; Hu et al. 2006). STV and colour variations have been investigated by many authors (e.g. Takalo et al. 1996; Gu et al. 2006; Rani et al. 2010a).

We observed 3C 66A for STV in 16 nights between 2009 November 13 and 2010 November 6. The source showed large flux variations, but no significant colour variations during our observing run (Fig. 1). The source showed a brightening trend by $\sim$0.5 mag in 38 d in the *R* band and again was as bright as 13.4 mag even after another 319 d (around JD 245 5505). This flux is comparable to the brightest *R* magnitude ($\sim$13.4) reported in the source by Böttcher et al. (2009). So we conclude that 3C 66A was in a high state during this period.

3.1.2 AO 0235+164

AO 0235+164 has a redshift of $z = 0.94$ based on the detection of emission lines (Nilsson et al. 1996) and was classified as a BL Lac object by Spinrad & Smith (1975). The synchrotron peak of this source is located at $10^{13.6}$ Hz and therefore it is classified as an LSP (Nieppola et al. 2006). This blazar has exhibited extreme variability (by over an order of magnitude on time-scales <1 yr) across all spectral ranges, including X-ray (Raiteri et al. 2009) and γ-ray (i.e., Abdo et al. 2010). It has been observed from the radio to X-ray bands on time-scales ranging from less than an hour to many years (e.g. Heidt & Wagner 1996; Fan & Lin 1999; Romero, Cellone & Combi 2000; Webb et al. 2000; Raiteri et al. 2001; Padovani et al. 2004). Raiteri et al. (2001) predicted that the blazar should show a possible correlated periodic radio and optical outburst on the time-scale of 5.7 ± 0.5 yr that was expected in 2004 February–March but that predicted outburst could not be detected (Raiteri et al. 2005, 2006a). Raiteri et al. (2006b) then reanalysed the long-term optical light curves and suggested that the optical outbursts may have a longer time-scale of $\sim$8 yr. Gupta et al. (2008) reported an outburst in 2007 January, with $R_{\rm mag} \simeq 14.98$ the peak seen during their observing run.

We have observed AO 0235+164 on eight nights between 2009 November 13 and 2010 November 6 and it showed significant flux as well as colour variations (Fig. 1). This source's magnitude varied between 17.9 and 18.3 mag in *R* band, and then was at $\sim$18.4 mag after $\sim$347 d (at JD 245 5508) which is $\sim$4 mag fainter than the brightest reported value for this source. We conclude that AO 0235+164 was probably in a low state in the period we observed it.

3.1.3 S5 0716+714

The blazar S5 0716+714 at redshift $z = 0.31 \pm 0.08$ is one of the most active sources in optical bands. Its optical UV continuum is so featureless (Biermann et al. 1981; Stickel, Fried & Kuehr 1993) that a redshift estimate has been possible only by resolving and using the host galaxy as a standard candle (Nilsson et al. 2008). This BL Lac is of the ISP type, displaying a first broad peak in the optical/UV bands and showing another broad peak near 1 GeV (Ferrero et al. 2006; Massaro et al. 2008). It is highly variable on time-scales from hours to months across all observed wavelengths (e.g. Wagner et al. 1990; Heidt & Wagner 1996; Villata et al. 2000; Raiteri et al. 2003; Foschini et al. 2006; Montagni et al. 2006; Ostorero et al. 2006; Gupta et al. 2008, and references therein). This source is one of the brightest BL Lacs in optical bands and has an IDV duty cycle of nearly 1 (e.g. Wagner et al. 1996; Montagni et al. 2006; Stalin et al. 2006). Gupta, Srivastava & Wiita (2009) analysed the excellent intraday optical LCs of the source obtained by Montagni et al. (2006) and reported some evidence for nearly periodic oscillations ranging between 25 and 73 min on several different nights. More recently, Rani et al. (2010b) reported very good evidence for a quasi-periodic oscillation of $\sim$15 min in a new optical light curve of S5 0716+714.

We observed S5 0716+714 on 19 nights between 2009 November 14 and 2011 March 25 for STV and in three nights in *R* passband (2010 December 11, 13 and 15) for IDV. This source exhibited significant STV and colour variations (Fig. 1). Also, the IDV light curves of the blazar and the differential instrumental magnitude of standard stars with arbitrary offset are displayed in Fig. 2. The source showed genuine IDV on all three nights and the visual impressions of the LCs were confirmed by *C*- and *F*-tests for those nights (Table 3). We performed SF and DCF analyses to find if any time-scale of variability was present in these nights (shown in Fig. 2) but no significant time-scale was found. There have been four major optical outbursts reported from S5 0716+714 at the

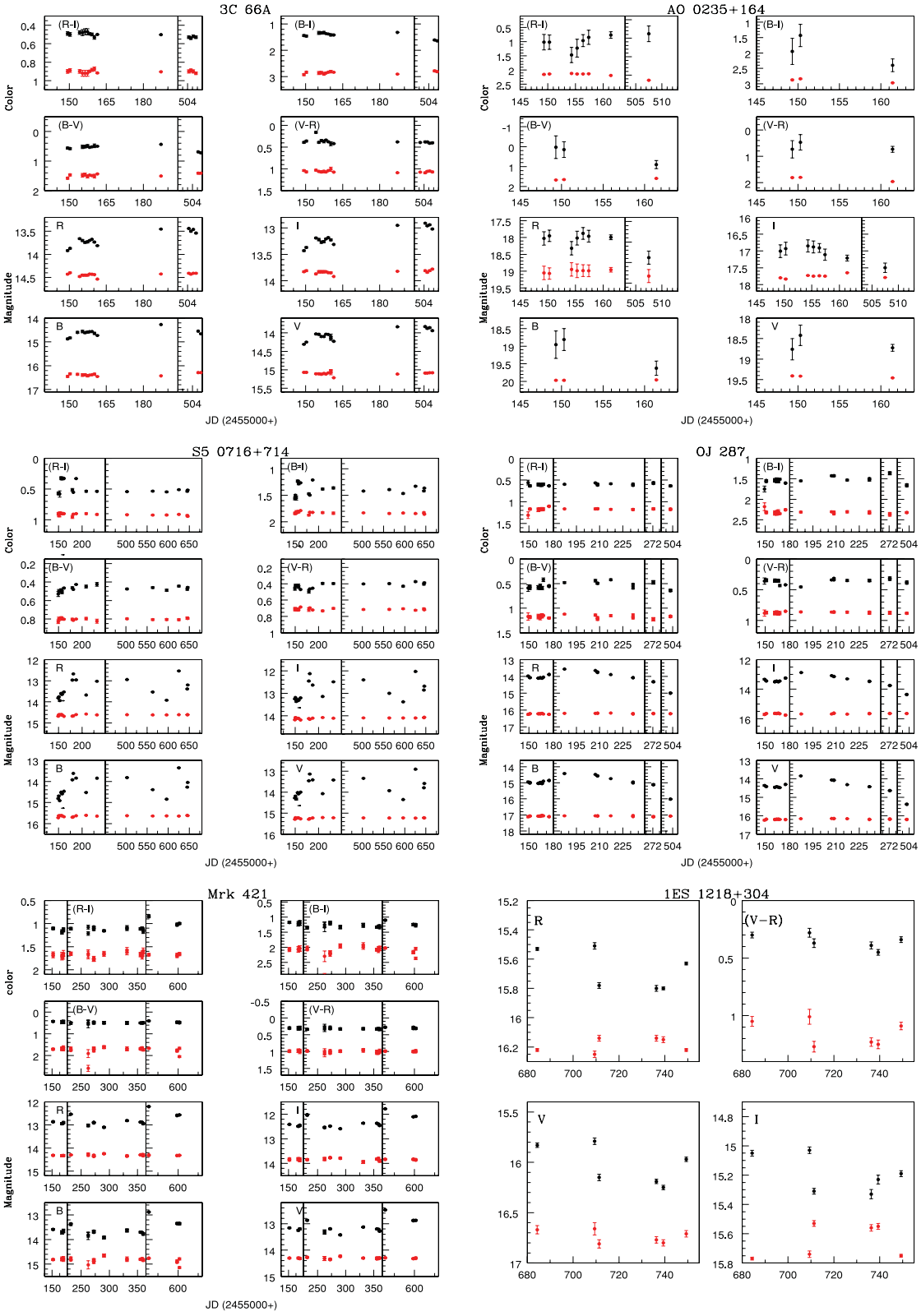

Figure 1. STV plots of blazars 3C 66A, AO 0235+164, S5 0716+714, OJ 287, Mrk 421 and 1ES 1218+304. For each source, the lower four panels show the calibrated LCs in B, V, R and I bands (upper LC), plotted with the differential instrumental magnitudes of standard stars with arbitrary offsets (lower LC). The corresponding colour LCs are plotted in upper four panels in $(B-V)$, $(V-R)$, $(R-I)$ and $(B-I)$.

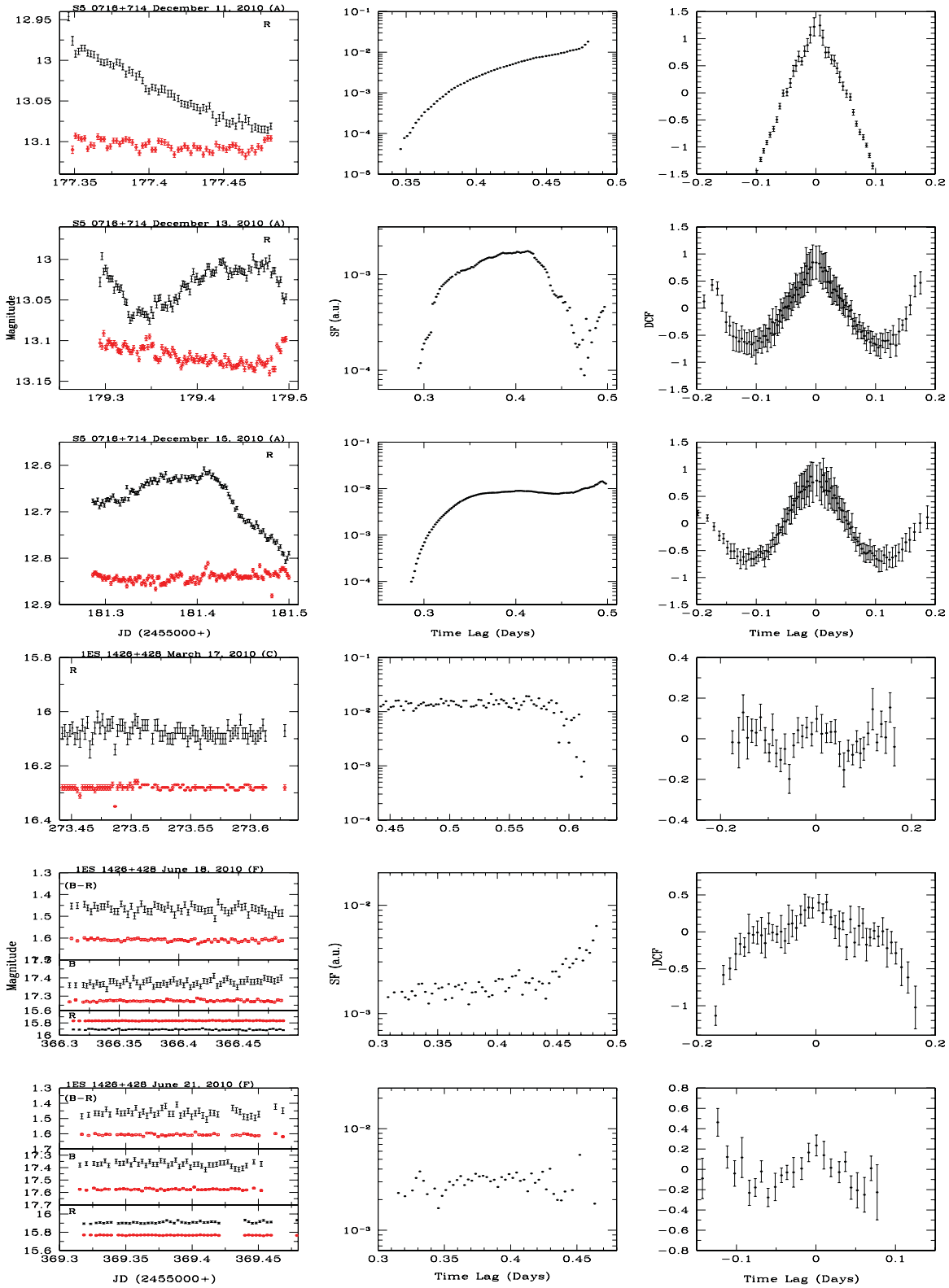

Figure 2. IDV light curves (upper panel is calibrated LC of blazar and lower panel is differential magnitude of standard stars) of S5 0716+714 and 1ES 1426+428 along with their SF and DCF (from left to right) using *R*-band data in each of the LCs.

beginning of 1995, in late 1997, in the fall of 2001 and in 2004 March (Raiteri et al. 2003; Foschini et al. 2006). These four outbursts give a possible period of long-term variability of $\sim 3.0 \pm 0.3$ yr. During our observations, the source first brightened by $\sim$1.15 mag in 32 d in the *R* band and then it fades by $\sim$1 mag over 27 d (covering the period JD 255 5149 to 245 5231). Later on, within 94 d this source faded by $\sim$0.98 mag (ending at JD 245 5596) and then again it brightened and reached the highest flux we saw at 12.54 mag at JD

Table 3. Results of IDV observations.

Source name	Date (dd.mm.yy)	Band	N	C-test C_1, C_2	F $F_1, F_2, F_c(0.99), F_c(0.999)$	Variable	A (per cent)
S5 0716+714	11.12.09	R	64	4.41, 4.62	19.44, 21.36, 1.81, 2.21	V	12.89
	13.12.09	R	104	2.07, 1.75	4.30, 3.06, 1.59, 1.85	PV	7.71
	15.12.09	R	115	4.85, 4.61	23.48, 21.27, 1.55, 1.79	V	18.19
OJ 287	22.11.09	R	35	1.37, 1.42	1.87, 2.01, 2.26, 2.98	NV	–
	21.12.09	R	129	0.96, 1.17	0.92, 1.36, 1.51, 1.73	NV	–
	10.01.10	R	90	0.85, 0.90	0.73, 0.81, 1.64, 1.94	NV	–
	11.01.10	R	80	1.03, 0.99	1.06, 0.98, 1.70, 2.02	NV	–
	20.01.10	R	62	1.04, 1.09	1.09, 1.20, 1.83, 2.24	NV	–
1ES 1426+428	15.03.10	R	31	0.64, 0.84	0.40, 0.71, 2.39, 3.22	NV	–
	17.03.10	R	83	4.62, 4.48	21.42, 20.09, 1.68, 2.00	V	11.99
	18.06.10	B	62	2.62, 2.34	6.88, 5.00, 1.83, 2.24	V	7.40
		R	62	2.00, 1.99	4.01, 3.94, 1.83, 2.24	PV	3.69
		$(B-R)$	62	2.51, 2.23	6.29, 4.96, 1.83, 2.24	V	7.70
	21.06.10	B	47	3.06, 2.80	9.38, 7.82, 2.01, 2.54	V	8.10
		R	59	3.14, 2.66	9.86, 7.09, 1.86, 2.28	V	4.10
		$(B-R)$	47	3.33, 3.17	11.11, 10.03, 2.01, 2.54	V	9.90
1ES 1553+113	07.05.10	R	111	0.51, 0.91	0.26, 0.83, 1.56, 1.81	NV	–
	11.06.10	R	120	0.78, 0.67	0.60, 0.45, 1.54, 1.74	NV	–
	12.06.10	B	50	0.57, 1.00	0.33, 1.00, 1.96, 2.46	NV	–
		R	50	0.47, 0.80	0.22, 0.64, 1.96, 2.46	NV	–
		$(B-R)$	50	0.54, 0.92	0.30, 0.84, 1.96, 2.46	NV	–
	14.06.10	B	24	0.97, 0.48	0.94, 0.23, 2.72, 3.85	NV	–
		R	21	1.01, 0.84	1.02, 0.70, 2.94, 4.29	NV	–
		$(B-R)$	21	0.96, 0.49	0.92, 0.24, 2.94, 4.29	NV	–
	20.06.10	B	61	0.70, 0.78	0.49, 0.61, 1.84, 2.25	NV	–
		R	61	0.78, 0.90	0.62, 0.82, 1.84, 2.25	NV	–
		$(B-R)$	61	0.67, 0.86	0.44, 0.74, 1.84, 2.25	NV	–
	21.06.10	B	57	0.88, 1.02	0.78, 1.04, 1.88, 2.32	NV	–
		R	57	0.70, 0.70	0.49, 0.49, 1.88, 2.32	NV	–
		$(B-R)$	57	0.81, 0.93	0.66, 0.86, 1.88, 2.32	NV	–

Note. V: variable; NV: non-variable; PV: possible variable.

245 5625. This is essentially as bright as ever reported in the earlier outbursts in the R passband (12.55 mag in the fall of 2001; Raiteri et al. 2003) and 12.55 mag in 2007 January (Gupta et al. 2008). We can conclude that the source was in an outburst state during our observing run.

3.1.4 OJ 287

OJ 287 is a LSP at redshift $z = 0.306$ (Sitko & Junkkarinen 1985) and has received a lot of attention as it has shown massive double-peaked outbursts approximately every 12 yr since the 1890s. Sillanpää et al. (1988) first noticed this exceptional behaviour and suggested that these outbursts might be caused by a close binary black hole system in which the secondary black hole induces tidal disturbances in the accretion disc of the primary black hole. Several other authors suggested models for OJ 287 (Katz 1997; Villata et al. 1998; Valtaoja et al. 2000), all of them based on the assumption that OJ 287 hosts a close binary black hole. It has been observed extensively in optical band (e.g. Carini & Miller 1992; Sillanpää et al. 1996a,b; Abraham 2000; Gupta et al. 2008; Fan et al. 2009). The observational properties of OJ 287 from radio to X-ray energy bands have been reviewed by Takalo, Sillanpaeae & Nilsson (1994). Fan et al. (2009) reported large variations in the source with $\Delta V = 1.96$ mag, $\Delta R = 2.36$ mag and $\Delta I = 1.95$ mag during their observations spanning 2002–2007. This quasar shows quasi-periodic optical outbursts at ∼12 yr intervals, with two outburst peaks per interval. Valtonen et al. (2008) discussed a model in which a secondary body (a black hole) pierces the accretion disc of the primary black hole and produces two impact flashes per period. This model predicted the next outbursts to occur between 2007 October and 2009 December and they were actually seen (Valtonen & Ciprini 2012 and references therein).

We observed OJ 287 on 16 nights between 2009 November 13 and 2010 November 2 for STV and on five nights between 2009 November 22 and 2010 January 20 for IDV. OJ 287 showed significant flux variations in all the observed passbands but no significant colour variations were found on short time-scales (Fig. 1). Furthermore, the IDV light curves of the source and the differential instrumental magnitude of two standard stars with arbitrary offset are displayed in Fig. 3. We performed C- and F-tests and found that the source did not show genuine IDV on any of the five nights. Real STV was certainly seen, as the source brightened by ∼0.6 mag in 38 d and peaked up to 13.56 mag in R band. Then, it faded to 15.01 mag in 317 d during our observing run. Pursimo et al. (2000) carried out multiband optical monitoring of the source for about 5 yr (1993–1998) and also plotted its V passband historical light curve for about century long observations. The 1993–1998 light curve of the source shows the brightest (∼13.5) and faintest (∼16.5 mag) states of the source in the R passband. In our present observations, we observed the source at $R \sim 13.56$ mag on JD 245 5187 in the R passband which is near to its brightest state. So, near 2009 December, the source was in outburst state and then faded by ∼1.54 mag by 2010 November.

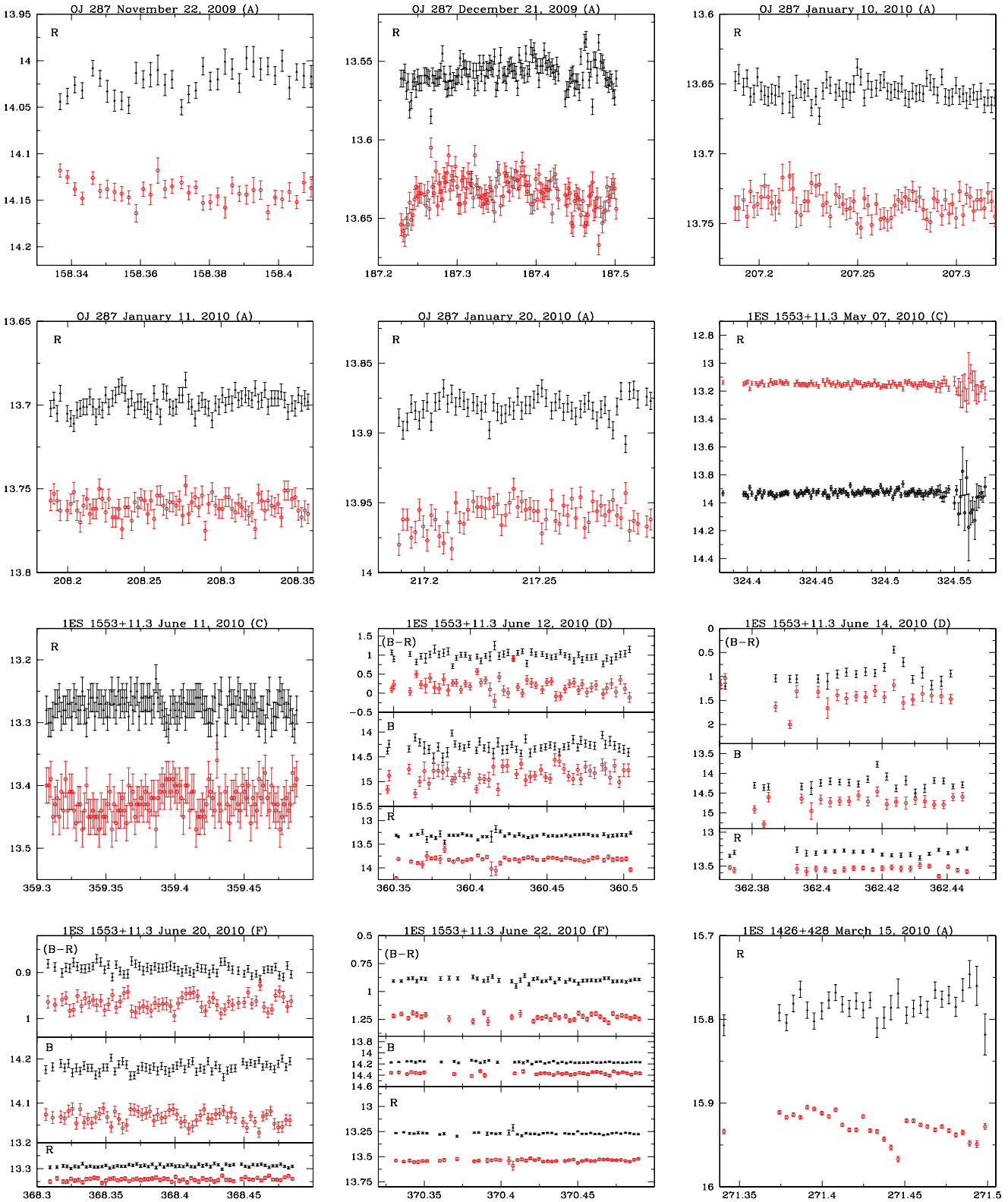

Figure 3. IDV light curves of the blazars OJ 287, 1ES 1553+113 and 1ES 1426+426. *X*-axis is JD(245 5000+) and *Y*-axis is magnitude in each figure. In each panel, upper curve (triangles) is the calibrated light curve of the blazar and the lower curve (open circles) is the differential light curve of the standard stars.

3.1.5 Mrk 421

Mrk 421 has $z = 0.031$ and is classified as an HSP because the energy of its synchrotron peak is higher than 0.1 keV. It is the brightest TeV γ-ray emitting blazar in the Northern hemisphere. It was first noticed to be an object with a blue excess which turned out to be an elliptical galaxy with a bright point like nucleus (Ulrich et al. 1975). It was the first known extragalactic TeV γ-ray emitter (Punch et al.

1992). It has been extensively observed at all wavelengths from radio to γ-rays. The source is characterized by strong variability in the optical region (i.e. Miller 1975; Liu, Liu & Xie 1997) including optical variations of at least 4.6 mag (Stein, Odell & Strittmatter 1976). Mrk 421 has been a target of several simultaneous multi-wavelength campaigns (Takahashi et al. 2000; Rebillot et al. 2006; Fossati et al. 2008; Lichti et al. 2008).

We observed Mrk 421 for STV on 17 nights between 2009 November 15 and 2011 May 2 in *B, V, R* and *I* bands. The flux from the nucleus of Mrk 421 is contaminated by the emission of the host galaxy so we used the measurements of Nilsson et al. (2007) to estimate the host galaxy emission in the *R* band. This flux is used to obtain the corresponding contribution for *B, V* and *I* bands (Fukugita, Shimasaku & Ichikawa 1995) and we corrected for the Galactic extinction using the extinction map of Schlegel, Finkbeiner & Davis (1998). The source showed genuine flux variations in the *V, R* and *I* bands, but no significant colour variations during our observing run (Fig. 1). During our observing run, the source showed an average brightness of ∼13.4 mag and reached a maximum brightness of ∼12.46 mag in the *V* band at around JD 245 5684 which is quite close to the maximum observed brightness of about $V \sim 12.0$ in 1996 November during an outburst (Tosti et al. 1998a). Thus we can say that this source was in an outburst state during our observing run.

3.1.6 1ES 1218+304

1ES 1218+304 has a redshift of 0.182 and was first detected to emit VHE γ-rays by Major Atmospheric Gamma-Ray Imaging Cherenkov (MAGIC) in 2005 (Albert et al. 2006). It is classified as an HSP as its synchrotron peak is located at $10^{19.14}$ Hz (Nieppola et al. 2006). In 2009 Very Energetic Radiation Imaging Telescope Array System (VERITAS) reported fast variability from the source, the peak flux reaching ∼26 per cent of the Crab nebula flux (Acciari et al. 2010).

We observed the source on six nights between 2011 March 2 and 2011 June 7 (Fig. 1). We performed *C*- and *F*-tests on these nights but neither STV nor colour variations were found for this source during our observations.

3.1.7 ON 231

ON 231 (also known as W Comae) was discovered in 1971 because of its odd properties, particularly a strong optical variability and an apparently lineless continuum (Biraud 1971; Browne 1971). The detection of weak emission lines in its spectrum made it possible to determine that its $z = 0.102$ (Weistrop et al. 1985). The historical *B* passband LC of the source (during 1935–1997) was plotted by Tosti et al. (1998b). It has shown optical flux variations on diverse time-scales ranging from a few hours to several years (Xie et al. 1992; Smith & Nair 1995). After the optical outburst, ON 231 showed a slow decline in its mean luminosity (Tosti et al. 2002). This source was also detected at high energies by Acciari et al. (2008).

We observed ON 231 for STV on 17 nights between 2009 November 15 and 2011 February 6 in *B, V, R* and *I* bands. The light curves of the calibrated blazar and differential instrumental magnitude of two standard stars with arbitrary offset are displayed in Fig. 4. During our observations ON 231 showed significant flux, but no significant colour, variations. Tosti et al. (1998b) carried out multi-band optical monitoring of the source for 3 yr (1994–1997) in its great outburst state and gave their brightest (∼13.5 mag) and faintest (∼15.0 mag) values in the *R* passband. In the present observations, the source brightened by ∼0.3 mag in the *R* passband over ∼11 d and peaked at 14.41 mag which is ∼0.6 mag fainter than the faintest state observed by the Tosti et al. (1998b). Then, the source faded to ∼15.08 mag at JD 245 5600. It appears likely we have observed ON 231 in a low state.

3.1.8 3C 279

The FSRQ 3C 279 shows flux variabilities at all frequencies. It is a LSP having synchrotron peak frequency at $10^{12.8}$ Hz (Planck Collaboration et al. 2011). Webb et al. (1990) reported rapid fluctuations of ∼2 mag within 24 h at visible wavelengths and a rapid variation of 1.17 mag within 40 min was seen in the *V* band (Xie et al. 1999). Gupta et al. (2008) reported a 1.5 mag variation in the *R* band over 42 d and Rani et al. (2010a) reported a rapid decay in the brightness of the source in 5 d by $\Delta R = 1.10$ mag. This source has been studied through multiwavelength campaigns (Hartman et al. 1996; Wehrle et al. 1998; Böttcher et al. 2007).

We observed 3C 279 on 11 nights between 2011 May 27 and 2011 June 24. We performed *C*- and *F*-tests (Table 4) on these nights and found genuine STV in *V*, *R* and *I* bands shown in Fig. 4. The source did not show genuine colour variations during the observations. In the *R* band, 3C 279 first faded by ∼0.47 mag in 16 d from 14.36 to 14.83 mag and then brightened again to 14.62 mag in 15 d. The source was reported to in outburst in 2007 January by Gupta et al. (2008) reaching a brightness of $R \sim 12.6$ mag and Rani et al. (2010a) have reported 17.1 mag as the faintest level in the source. So we can say that 3C 279 was in either a pre- or post-outburst state during our observations.

3.1.9 1ES 1426+428

The blazar 1ES 1426+428 was discovered in the medium X-ray band (2–6 keV) with the Large Area Sky Survey Experiment (LASS) on the first of the *High Energy Astronomy Observatories* (Wood et al. 1984). The host galaxy of 1ES 1426+426 was resolved by Urry et al. (2000) and found to have $m_R = 16.14$, leading to a photometric redshift of $z = 0.132 \pm 0.030$. It was classified as a BL Lac object because of its lack of prominent optical emission lines by Remillard et al. (1989). Based on observations by *BeppoSAX* up to 100 keV, 1ES 1426+428 is an example of an extreme-high-energy-peaked BL Lac object (HSP) with the peak of the synchrotron emission lying above 100 keV (Costamante et al. 2001) during that observing campaign. Hence it was a prime candidate for TeV γ-ray emission, which was confirmed by the Whipple Collaborations (Petry et al. 2000; Horan et al. 2002). Optical polarization and photometry of the source was done by Jannuzi, Smith & Elston (1993, 1994).

We observed 1ES 1426+428 for STV on 14 nights between 2010 March 16 and 2011 February 8 out of which we observed the source for IDV on four nights (2009 March 15, 17 and 2010 June 18, 21). We found genuine STV and colour variation in this source. The light curve of the source for STV and its colour variations are shown in Fig. 4. IDV light curves of the blazar and the differential instrumental magnitudes are displayed in Fig. 2. For two nights (2010 June 18 and 21), we have observed the source quasi-simultaneously in the *B* and *R* bands. The source showed genuine IDV during three nights which are confirmed by *C*- and *F*-tests for these nights. We performed SF and DCF analyses to search for any time-scales of variability but no significant time-scale was found. During our observing run, the source showed an average magnitude of ∼15.9 in the *R* band. In last decade, the source has only varied between

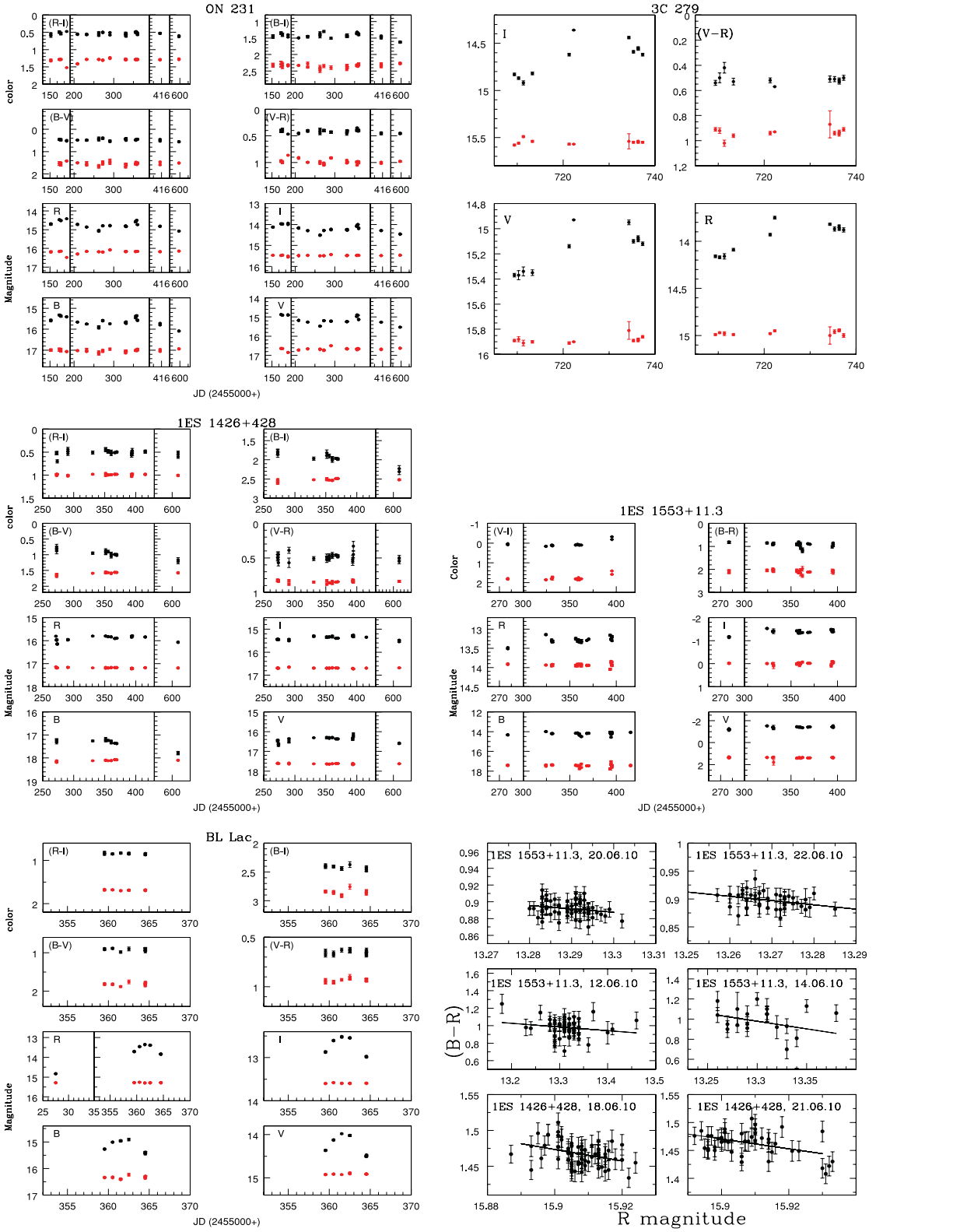

Figure 4. As in Fig. 1 for STV plots of ON 231, 3C 279, 1ES 1426+428, 1ES 1553+11.3 and BL Lac. The lower right-hand panel shows the colour variation ($B - R$) versus R magnitude on intraday time-scales with the source and respective date noted in each subpanel.

∼15.7 and 16.1 mag.[3] So, the source in our observations also shows a similar state of brightness.

3.1.10 1ES 1553+113

1ES 1553+113 was discovered in The Palomar–Green Survey of UV-excess objects as a 15.5 mag blue stellar object (Green, Schmidt

[3] http://users.utu.fi/kani/1m/

Table 4. Results of STV observations.

Source name	Band	N	C-test C_1, C_2	F $F_1, F_2, F_c(0.99), F_c(0.999)$	Variable	A (per cent)
3C 66A	B	13	2.80, 2.95	7.81, 8.71, 4.16, 7.00	V	53.90
	V	15	4.15, 3.95	17.21, 15.62, 3.70, 5.93	V	43.51
	R	15	5.05, 4.60	25.46, 21.19, 3.70, 5.93	V	43.50
	I	15	5.69, 5.27	32.38, 27.75, 3.70, 5.93	V	46.98
	$(B-V)$	12	7.25, 7.73	52.63, 59.82, 4.46, 7.76	V	26.10
	$(B-I)$	12	1.78, 2.38	3.17, 5.67, 4.46, 7.76	NV	–
	$(V-R)$	15	1.68, 1.77	2.83, 3.14, 3.70, 5.93	NV	–
	$(R-I)$	15	1.22, 0.79	1.49, 0.63, 3.70, 5.93	NV	–
AO 0235+164	B	6	42.41. 43.19	179.94, 186.13, 10.97, 29.75	V	92.52
	V	6	7.88, 7.56	62.16, 57.11, 10.97, 29.75	V	49.60
	R	14	3.68, 3.51	13.56, 12.31, 3.91, 6.41	V	57.30
	I	16	4.21. 4.32	17.75, 18.65, 3.52, 5.54	V	79.23
	$(B-V)$	6	9.38, 10.19	88.07, 103.81, 10.97, 29.75	V	79.54
	$(B-I)$	6	6.10, 5.27	37.16, 27.75, 10.97, 29.75	V	71.25
	$(V-R)$	6	3.10, 2.50	9.63, 6.23, 10.97, 29.75	V	58.18
	$(R-I)$	14	13.43, 13.59	180.30, 184.73, 3.91, 6.41	V	70.93
S5 0716+714	B	18	14.52, 14.60	210.83, 213.19, 3.24, 4.92	V	122.96
	V	18	17.96, 17.97	322.69, 322.99, 3.24, 4.92	V	116.34
	R	18	2.25, 1.88	5.04, 3.52, 3.24, 4.92	V	112.87
	I	18	13.59, 13.50	184.63, 182.14, 3.24, 4.92	V	110.59
	$(B-V)$	18	2.92, 3.05	8.54, 9.30, 3.24, 4.92	V	14.25
	$(B-I)$	18	6.18, 5.65	38.21, 31.89, 3.24, 4.92	V	31.96
	$(V-R)$	18	2.35, 1.36	5.52, 1.85, 3.24, 4.92	V	75.79
	$(R-I)$	12	5.23, 4.72	27.38, 22.32, 4.46, 7.76	V	21.38
OJ 287	B	22	5.99, 6.40	35.88, 40.98, 2.86, 4.13	V	117.31
	V	22	12.17, 12.08	148.17, 145.95, 2.86, 4.13	V	107.94
	R	22	4.82, 4.89	23.22, 23.92, 2.86, 4.13	V	105.77
	I	21	8.41, 8.59	70,73, 73.74, 2.94, 4.29	V	102.89
	$(B-V)$	20	0.55, 1.47	0.30, 2.17, 3.03, 4.47	NV	–
	$(B-I)$	20	1.09, 1.74	1.89, 3.02, 3.03, 4.47	NV	–
	$(V-R)$	22	1.11, 0.55	1.24, 0.30, 2.86, 4.13	NV	–
	$(R-I)$	21	0.65, 0.58	0.43, 0.37, 2.94, 4.29	NV	–
Mrk 421	B	29	1.75, 1.35	3.05, 1.82, 2.46, 3.36	NV	–
	V	29	8.10, 8.06	65.68, 64.92, 2.46, 3.36	V	95.38
	R	33	7.21, 6.94	51.93, 48.15, 2.32, 3.09	V	91.28
	I	35	4.25, 4.50	18.04, 20.29, 2.26, 2.98	V	81.60
	$(B-V)$	29	1.02, 0.17	1.04, 0.03, 2.46, 3.36	NV	–
	$(B-I)$	29	1.04, 0.37	1.09, 0.13, 2.46, 3.36	NV	–
	$(V-R)$	29	1.12, 0.79	1.24, 0.61, 2.46, 3.36	NV	–
	$(R-I)$	33	0.97, 0.54	0.95, 0.30, 2.32, 3.09	NV	–
1ES 1218−304	V	6	1.26, 0.68	1.58, 0.46, 10.97, 29.75	NV	–
	R	6	0.75, 1.16	0.56, 1.34, 10.97, 29.75	NV	–
	I	6	0.63, 1.04	1.00, 0.09, 10.97, 29.75	NV	–
	$(V-R)$	6	0.98, 0.30	1.00, 0.09, 10.97, 29.75	NV	–
	$(R-I)$	6	1.78, 1.17	3.18, 1.37, 10.97, 29.75	NV	–
ON 231	B	34	2.57, 2.45	6.62, 5.98, 2.29, 3.04	V	65.64
	V	33	2.83, 2.88	8.00, 8.27, 2.32, 3.09	V	133.47
	R	35	2.64, 2.70	6.96, 7.29, 2.26, 2.98	V	173.44
	I	37	7.74, 7.80	59.89, 60.84, 2.20, 2.89	V	159.48
	$(B-V)$	32	0.90, 0.65	0.82, 0.43, 2.35, 3.15	NV	–
	$(B-I)$	32	1.19, 1.10	1.41, 1.21, 2.35, 3.15	NV	–
	$(V-R)$	31	0.79, 0.73	0.63, 0.54, 2.39, 3.22	NV	–
	$(R-I)$	17	1.60, 1.52	2.57, 2.30, 3.37, 5.20	NV	–
3C 279	V	11	6.30, 5.81	39.68, 33.75, 4.85, 8.75	V	43.84
	R	11	7.41, 7.66	54.96, 58.73, 4.85, 8.75	V	55.86
	I	11	7.80, 7.38	60.83, 54.45, 4.85, 8.75	V	41.81
	$(V-R)$	11	0.94, 0.99	0.88, 0.98, 4.85, 8.75	NV	–
	$(R-I)$	11	1.28, 1.41	1.64, 1.98, 4.85, 8.75	NV	–
1ES 1426+428	B	15	5.26, 5.48	27.70, 30.05, 3.70, 5.93	V	60.89
	V	24	6.68, 7.09	44.67, 50.23, 2.72, 3.85	V	57.96
	R	27	5.73, 5.73	32.88, 32.84, 2.55, 3.53	V	36.99
	I	31	4.08, 4.46	16.63, 19.87, 2.39, 3.22	V	28.97

Table 4 – *continued*

Source name	Band	N	C-test C_1, C_2	F $F_1, F_2, F_c(0.99), F_c(0.999)$	Variable	A (per cent)
	$(B-V)$	15	2.63, 3.13	6.93, 9.81, 3.70, 5.93	V	45.83
	$(B-I)$	15	4.17, 4.37	17.36, 19.14, 3.70, 5.93	V	50.87
	$(V-R)$	24	3.06, 3.27	9.38, 10.68, 2.72, 3.85	V	23.88
	$(R-I)$	24	3.89, 3.70	15.17, 13.66, 2.72, 3.85	V	25.94
1ES 1553+113	B	36	0.65, 1.05	0.43, 1.11, 2.23, 2.93	NV	–
	V	32	1.74, 0.75	3.01, 0.57, 2.35, 3.15	NV	–
	R	34	1.38, 1.15	1.91, 1.32, 2.29, 3.04	NV	–
	I	30	1.98, 1.96	3.94, 3.83, 2.42, 3.29	NV	–
	$(B-R)$	31	0.48, 1.08	0.23, 1.18, 2.39, 3.22	NV	–
	$(V-I)$	28	1.73, 0.73	2.98, 0.54, 2.51, 3.44	NV	–
BL Lac	B	16	3.46, 3.41	11.96, 11.61, 3.52, 5.54	V	51.33
	V	14	16.90, 16.68	285.44, 278.34, 3.91, 6.41	V	50.46
	R	16	42.04, 41.95	1767.69, 1760.03, 3.52, 5.54	V	119.04
	I	12	25.92, 25.78	672.10, 664.80, 4.46, 7.76	V	43.51
	$(B-V)$	14	0.76, 0.76	0.57, 0.58, 3.91, 6.41	NV	–
	$(B-I)$	12	0.57, 0.70	0.32, 0.49, 4.46, 7.76	NV	–
	$(V-R)$	14	1.40, 0.90	1.96, 0.81, 3.91, 6.41	NV	–
	$(R-I)$	12	1.79, 1.73	3.20, 2.99, 4.46, 7.76	NV	–

Note. V: variable; NV: non-variable.

& Liebert 1986) and BL Lac classification was suggested by the featureless spectrum (Miller & Green 1983) with an optical R magnitude varying from ∼13 to ∼15.5 (Miller et al. 1988). Its SED indicates that it is an HSP (Falomo & Treves 1990; Donato, Sambruna & Gliozzi 2005). The logarithmic ratio of its 5 GHz radio flux, $F_{5\,\mathrm{GHz}}$, to its 2 keV X-ray flux, $F_{2\,\mathrm{keV}}$, has been found to range from $\log(F_{2\,\mathrm{keV}}/F_{5\,\mathrm{GHz}}) = -4.99$ to -3.88 (Rector, Gabuzda & Stocke 2003; Osterman et al. 2006). 1ES 1553+113 has been detected from radio through hard X-rays and also in the VHE ($E \geq 100$ GeV) bands up to energies above 1 TeV (Aharonian et al. 2006; Albert et al. 2007). It is in the *Fermi* Large Area Telescope (LAT) Bright AGN source list (LBAS; Abdo et al. 2009).

It is a bright optical source with V-band magnitude of $V \sim 14$ (Falomo & Treves 1990; Osterman et al. 2006). Observations taken between 1986 and 1991 found its optical spectral index, α_O, to remain constant ($\alpha_O \sim -1$) and its magnitude to vary by $\Delta V = 1.4$ (Falomo, Scarpa & Bersanelli 1994).

We observed 1ES 1553+113 for STV on 15 nights between 2010 March 18 and 2010 August 6 and in six nights for IDV (between 2010 May 7 and 2010 June 21). In four out of these six nights, we observed the source in B and R bands quasi-simultaneously and also searched for colour variations in $(B-R)$ band on intraday timescales (Fig. 3). We performed C- and F-tests in all nights but genuine IDV was not found during any night. Furthermore, colour variations in $(B-R)$ were not found on these four nights. Genuine STV was found but the source exhibited no significant colour variations (Fig. 4). During our observing run, the source exhibited the average magnitude of ∼13.3 mag in R band. This value is even higher than the brightest earlier measurement (13.5 mag) observed by Osterman et al. (2006) during the flaring state of source. So we clearly have observed this source in a high state.

3.1.11 BL Lac

BL Lac (2200+420), lies in an elliptical galaxy at a redshift of ∼0.07 (Miller, French & Hawley 1978). It is classified as a LSP (Fossati et al. 1998). BL Lac has been studied in detail during various intensive multiwavelength campaigns (Madejski et al. 1999; Villata et al. 2002; Böttcher et al. 2003; Ravasio et al. 2003 and references therein). Fan et al. (1998) presented historical optical data (in *UBVRI*) over ∼100 yr covering the period 1896–1996 and found large variations in all the bands.

We observed this prototypical source on six nights between 2009 July 15 and 2010 June 17. BL Lac exhibited significant flux variations but no colour variations during our observing period. In the R band, the source was in a low state at 14.83 mag on JD 245 5027 which is quite close to the faintest value (14.91 mag) mentioned in Fan & Lin (2000). During our observations on 5 d (2010 June 12–17) source showed the average magnitude of ∼13.40 mag in R band which is only ∼1.5 mag brighter than the faintest mag reported for the source by Fan & Lin (2000). So it is fair to say that the source was in a low state during our observing run.

3.2 Correlated variations between colour and magnitude

We have seen the corresponding variations in the $(B-V)$, $(V-R)$, $(R-I)$ and $(B-I)$ colour indices of these blazars with respect to variations in brightness. Colour–magnitude plots of the individual sources are displayed in Fig. 5. The individual panels show the $(B-V)$, $(V-R)$, $(R-I)$ and $(B-I)$ colours plotted (in sequence from bottom to top with arbitrary offsets) with respect to V magnitude. The straight lines shown are the best linear fit for each of the colour indices, Y, against magnitude, V, for each of the sources: $Y = mV + c$. Fitted values for the slopes of the curves, m, and the constants, c, are listed in Tables 5 and 6. We have also quoted the linear Pearson correlation coefficients, r, and the corresponding null hypothesis probability values, p.

A positive correlation here is defined as a positive slope between the colour index and apparent magnitude of the blazar. This means that the source tends to be bluer when it brightens or redder when it dims. An opposite correlation (with negative slope) implies the source follows a redder when brighter behaviour.

We found significant positive correlations ($p \leq 0.05$) between the V magnitude and some of the colour indices for the blazars: S5 0716+714 $(B-V)$; OJ 287 $(B-V)$; Mrk 421 $(B-V)$, $(R-I)$, $(B-I)$, ON 231 $(V-R)$, $(R-I)$, $(B-I)$ and 1ES 1426+428

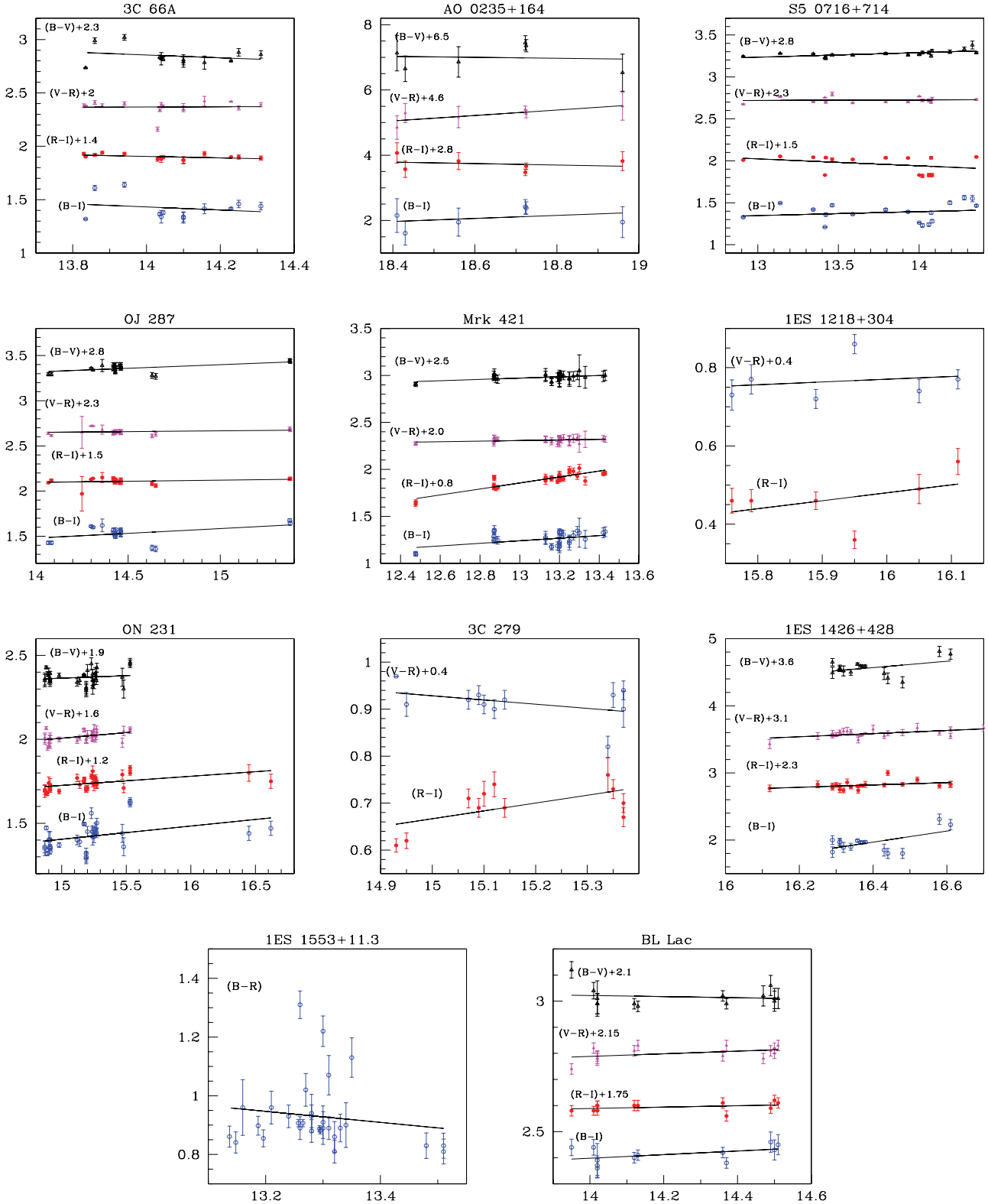

Figure 5. Colour–magnitude plots of blazars on short-term time-scales. *X*-axis is colour and *Y*-axis is *V* magnitude in each figure. For 1ES 1553+113, *Y*-axis is *R* magnitude.

$(V - R)$, $(B - I)$. AO 0235+164 $(V - R)$ showed a weak positive correlation. No significant negative correlations are found for any source. 3C 66A, 1ES 1218+304, 3C 279 and BL Lac lacked any significant correlations greater than 95 per cent confidence. For 1ES 1553+113, we found variations of $(B - R)$ colour with respect to V magnitude but the linear Pearson correlation coefficient, $r = -0.146$ gives a $p = 0.441$; hence, no significant correlation is found for this source.

Table 5. Fits to colour–magnitude dependences and colour–magnitude correlation coefficients on intraday time-scale.

Source name	Date (dd.mm.yy)	$(B-R)$ versus R m^a	c^a
		r^a	p^a
1ES 1426+428	18.06.10	−0.755	13.473
		−0.342	0.0065
	21.06.10	−0.821	14.529
		−0.422	0.0039
1ES 1553+113	12.06.10	−0.425	6.642
		−0.180	0.211
	14.06.10	−1.510	21.069
		−0.281	0.231
	20.06.10	−0.402	6.238
		−0.228	0.078
	22.06.10	−0.898	12.812
		−0.622	3.894e-06

[a]m = slope; c = intercept of CI against V; r = Pearson coefficient; p = null hypothesis probability.

4 THE OPTICAL SPECTRAL SLOPE DISTRIBUTION

We have combined the optical data in the *B, V, R* and *I* bands from our present observations with optical observations of three more sources: two HSPs (1ES 1959+650 and 1ES 2344+514) and one LSP (3C 454.3) from our papers Gaur, Gupta & Wiita (2012a) and Gaur et al. (2012b), respectively. We cannot use 1ES 1553+113 in this aspect of our study as the standard stars in its field are available only in the *B* and *R* bands. We regard these quasi-simultaneous multiband observations taken within 30 min as 'simultaneous' observations (Fiorucci, Ciprini & Tosti 2004), but we caution that occasionally a significant variation will have occurred between the measurements at different bands. All the observational data in the *B, V, R* and *I* bands were corrected for foreground Galactic interstellar reddening, which is deduced from the maps of dust infrared emission reported by Schlegel et al. (1998).

The radiation of these blazars can be adequately described by a single power law $F_\nu = A\nu^{-\alpha}$ in the optical band, where α is the spectral slope which is obtained by using the linear least-square fitting between log F_ν and log ν. In no case do we measure significant curvature to the spectra. We have accepted only the data that allow us to calculate the regression based on at least three quasi-simultaneous photometric bands, and whose square of Pearson's linear correlation coefficient is greater than 0.9. Furthermore, the standard deviation of the fitted slope must be less than 0.25 for us to consider the fit valid. These selection criteria assure the accuracy of the slopes by cutting out all the sets of three or four data points that contain at least one wrong value (Hu et al. 2006). These results are listed in Table 7. Our sample consists of six LSPs, three ISPs and six HSPs. The sequence of columns in Table 7 is the following: the source name; each photometric band average flux density (in mJy) and the number of useful data points; the average optical spectral index α, the standard deviation of α and the number of data points; the variation amplitude (max–min) of the optical spectral slope M_α; the slope of the linear regression between α and the *R* magnitude, b, and its standard deviation; the correlation coefficient between α and *R* magnitude and the corresponding p values.

5 DISCUSSION

5.1 Flux variations

5.1.1 Intraday and short-term variability time-scales

We carried out photometric observations of four blazars S5 0716+714, OJ 287, 1ES 1426+428 and 1ES 1553+113 for IDV in the *R* band. For some of these nights, we have carried

Table 6. Fits to colour–magnitude dependences and colour–magnitude correlation coefficients on short time-scale.

Source name	$(B-V)$ versus V m^a	c^a	$(V-R)$ versus V m	c	$(R-I)$ versus V m	c	$(B-I)$ versus V m	c
	r^a	p^a	r	p	r	p	r	p
3C 66A	−0.131	4.689	0.012	2.199	−0.068	2.856	−0.141	3.412
	−0.233	0.467	0.030	0.917	−0.450	0.092	−0.199	0.535
AO 0235+164	−0.145	9.702	0.838	−10.368	−0.222	7.883	0.470	−6.683
	−0.081	0.879	0.778	0.068	−0.218	0.678	0.322	0.534
S5 0716+714	0.055	2.517	0.006	2.643	−0.083	3.104	0.046	0.744
	0.639	0.004	0.070	0.804	−0.341	0.213	0.183	0.468
OJ 287	0.081	2.190	0.018	2.401	0.024	1.758	0.106	−0.004
	0.545	0.016	0.207	0.381	0.205	0.386	0.418	0.075
Mrk 421	0.137	−0.541	0.031	−0.100	0.317	−3.065	0.137	−0.541
	0.454	0.013	0.337	0.0736	0.872	6.925e-10	0.454	0.013
1ES 1218+304	*	*	−0.089	1.872	0.167	−1.832	*	*
	*	*	−0.400	0.223	0.590	0.057	*	*
ON 231	0.030	1.921	0.066	1.010	0.054	0.911	0.079	0.225
	0.001	0.461	0.440	0.013	0.518	0.002	0.374	0.029
3C 279	*	*	0.071	−0.358	0.203	−2.770	*	*
	*	*	0.193	0.714	0.44	0.383	*	*
1ES 1426+428	0.467	−6.694	0.2357	−3.38	0.176	−2.37	0.821	−11.502
	0.386	0.156	0.577	0.0031	0.386	0.076	0.569	0.027
BL Lac	−0.021	3.322	0.050	2.090	0.026	2.220	0.069	1.434
	−0.131	0.655	0.436	0.119	0.345	0.272	0.461	0.131

[a]m = slope; c = intercept of CI against V; r = Pearson coefficient; p = null hypothesis probability.
*Missing entry is due to lack of data.

Table 7. Flux density and spectral slope in the optical region.

Source	Class	B (mJy)		V (mJy)		R (mJy)		I (mJy)		α		M_α	$b(\pm\sigma)$	r	p
		Avg	N	Avg	N	Avg	N	Avg	N	Avg	N				
3C 66A	ISP	8.13	13	11.42	15	13.02	15	15.41	15	1.01 ± 0.15	15	0.48	0.007 ± 0.022	0.087	0.756
J0211+1051	LSP	8.57	3	9.89	4	11.24	4	15.78	4	1.13 ± 0.12	4	0.27	-0.051 ± 0.049	−0.585	0.415
AO 0235+164	LSP	0.13	2	0.17	2	0.24	2	0.42	2	2.08 ± 0.62	2	*	*	*	*
S5 0716+714	ISP	9.73	18	13.06	18	15.92	18	19.34	18	1.20 ± 0.16	18	0.52	-0.003 ± 0.006	−0.112	0.657
1ES 0806+524	HSP	4.05	3	4.61	4	5.10	4	5.79	4	0.63 ± 0.02	4	0.05	-0.130 ± 0.032	−0.945	0.054
OJ 287	LSP	4.47	10	6.59	10	7.56	10	10.16	10	1.41 ± 0.14	10	0.44	-0.016 ± 0.024	−0.229	0.524
Mrk 421	HSP	15.38	29	21.31	29	25.15	29	30.86	29	1.08 ± 0.12	29	0.39	0.010 ± 0.007	0.417	0.156
	–[a]	14.05	29	16.63	29	18.97	29	*	*	0.62 ± 0.15	29	0.52	0.011 ± 0.007	0.416	0.156
1ES 1218+304	HSP	*	*	1.16	6	1.19	6	2.31	6	0.89 ± 0.14	6	0.38	-0.356 ± 0.216	−0.635	0.175
ON 231	ISP	2.57	16	3.32	16	4.26	16	5.37	16	1.30 ± 0.14	16	0.53	-0.083 ± 0.041	−0.474	0.064
3C 279	LSP[b]	2.26	4	3.53	11	4.70	11	6.88	11	1.13 ± 0.14	11	0.48	-0.080 ± 0.060	−0.418	0.200
1ES 1426+428	HSP	*	*	1.053	10	1.38	10	1.74	10	1.36 ± 0.21	10	0.73	-0.893 ± 0.390	−0.624	0.051
	–[a]	*	*	0.572	3	0.641	3	0.650	3	0.33 ± 0.14	3	*	*	*	*
BL Lac	LSP	13.55	5	20.26	5	26.72	5	36.29	5	1.69 ± 0.04	5	0.11	-0.004 ± 0.005	−0.432	0.467
1ES 1959+650	HSP	5.16	32	6.87	32	7.54	32	8.89	32	1.03 ± 0.23	32	1.08	-0.060 ± 0.018	−0.526	0.002
	–[a]	4.26	29	5.20	29	5.31	29	5.92	29	0.67 ± 0.15	29	0.59	-0.055 ± 0.011	−0.710	1.613×10^{-5}
3C 454.3	LSP[b]	3.36	32	4.91	31	6.18	32	13.38	6	1.47 ± 0.20	32	0.88	0.071 ± 0.012	0.741	1.216×10^{-6}
1ES 2344+514	HSP	*	*	3.51	30	5.35	30	7.45	30	1.77 ± 0.32	30	1.16	-0.271 ± 0.056	−0.674	4.388×10^{-5}
	–[a]	*	*	1.32	27	2.10	27	2.77	27	1.61 ± 0.29	27	1.27	-0.096 ± 0.088	−0.212	0.288

*Missing entry is due to lack of data.
[a]Data corrected for host galaxy contribution.
[b]Also a FSRQ.

out quasi-simultaneous observations in B and R passbands for 1ES 1426+428 and 1ES 1553+113. IDV was not detected for OJ 287 and 1ES 1553+113 during any night as seen in Fig. 3. For two other sources, S5 0716+714 and 1ES 1426+428, we found genuine IDV in 2 (out of 3) and in 4 (out of 5) nights, respectively (shown in Fig. 2). We searched for time-scales of variability using SF and DCF techniques, but no significant variability of time-scale was found for any of these blazars.

We performed photometric observations of nine blazars in the *BVRI* passbands during our observing run covering the period 2009–2011. Comparisons of our observations with earlier measurements of the same sources indicated that the blazars 3C 66A, S5 0716+714, OJ 287, Mrk 421 and 1ES 1553+113 were probably in high states; blazars AO 0235+164, ON 231 and BL Lac were apparently in faint states and 3C 279 was in a pre- or post-outburst state. The substantial flux variations for optical IDV and STV in blazars can be reasonably explained by models involving relativistic shocks propagating outwards (e.g. Marscher & Gear 1985; Wagner & Witzel 1995; Marscher 1996), although most of the IDV in the radio band comes from interstellar scattering. The larger flares are expected to be produced by the emergence and motion of a new shock triggered by some strong variations in a physical quantity such as velocity, electron density or magnetic field moving into and through the relativistic jet. IDV reported in the blazars is generally attributed to the shock moving down the inhomogeneous medium in the jet. In AO 0235+164, gravitational microlensing (e.g. Gopal-Krishna & Subramanian 1991) may play a role as it is known to have two galaxies (at $z = 0.524$ and 0.851) along our line of sight to it.

5.2 Colour variations

We have reported searches for variations in colour with time for time periods corresponding to STV in a sample of blazars. Out of 11 blazars we have newly observed, only three (AO 0235+164, S5 0716+714 and 1ES 1426+421) have shown significant colour variations on short time-scales. Phenomena that could lead to colour variations with time were summarized by Hawkins (2002) who noted they could arise from colour changes in accretion discs, different contributions from the underlying host galaxy arising from changes in seeing and colour changes from microlensing.

Colour variations in these sources are most unlikely to arise from the underlying host galaxy, as in the case of BL Lacs, Doppler boosted jet emission almost invariably swamps the light from the host galaxy. Furthermore, BL Lacs seem to have much weaker disc emission, so colour changes arising in the accretion disc are also unlikely. AO 0235+164 showed significant colour variations and is known to have two foreground galaxies at $z = 0.524$ and 0.851 (Nilsson et al. 1996) so colour variations seen in this source could arise from microlensing of different regions within a relativistic jet (Gopal-Krishna & Subramanian 1991). In the case of BL Lacs, any accretion disc radiation is always overwhelmed by that from the jet, and therefore jet models that can produce different fluctuations in different colours are most likely to be able to explain the colour variations we have detected. In the usual models involving shocks propagating down the jets (e.g. Marscher & Gear 1985; Marscher et al. 2008), radiation at different frequencies is produced at different distances behind the shocks. Higher frequency photons from the synchrotron component emerge sooner and closer to the shock front. Hence colour variations in blazars could arise from differences in the times and rates at which radiation observed at different visible colours rise and fall.

5.3 Relation between colour index and flux variation

We now investigate the relationship between spectral changes and flux variations on short term as well as intraday time-scales. On short time-scales, out of the 11 blazars for which new data are presented here, five (S5 0716+714, OJ 287, Mrk 421, ON 231 and 1ES 1426+428) have shown significant positive correlation

between colour and magnitude; one (AO 0235+164) has shown a very weak positive correlation, while five (3C 66A, 1ES 1218+304, 3C 279, BL Lac and 1ES 1553+113) lacked any correlation.

No significant negative correlation was found for any BL Lac which reflects the common trend for this class that they become bluer when they brighten (Ghisellini et al. 1997; Fan et al. 1998; Massaro et al. 1998; Fan & Lin 1999; Ghosh et al. 2000; Raiteri et al. 2001; Villata et al. 2002; Gu et al. 2006; Rani et al. 2010a). It has been found that the amplitude of the variations is systematically larger at higher frequencies, which suggests that the spectrum becomes steeper when the source brightness decreases, and flatter when it increases (Ghisellini et al. 1997; Massaro et al. 1998). The variations of the colour indices of our BL Lac objects follow this trend. It is possible to explain this colour variation with a one-component synchrotron model, i.e. the more intense the energy release, the higher the typical particle's energy and the higher the corresponding frequency (Fiorucci et al. 2004). It could also be explained if the luminosity increase was due to the injection of fresh electrons with an energy distribution harder than that of the previous, partially cooled ones (e.g. Kirk, Rieger & Mastichiadis 1998; Mastichiadis & Kirk 2002). However, some evidence that the amplitudes of variations are not systematically larger at high frequencies has been found on several occasions (Brown et al. 1989; Massaro et al. 1998; Ghosh et al. 2000; Ramírez et al. 2004). Ghosh et al. (2000) suggested that it may not be correct to generalize that the amplitude of the variation in blazars is systematically larger at higher frequency as they found a reddening as the brightness increases in their optical observations of the BL Lac objects PKS 0735+178, 3C 66A and AO 0235+164.

The trend of steeper spectra when brighter seems to generally hold for the variations we saw in IDV. On intraday time-scales, 1ES 1426+428 and 1ES 1553+113 (during 1 night) showed significant negative correlations between colour index and magnitude. So we can say that the trend of flatter spectra when brighter does not always hold for variations on time-scales of days. While amplitudes of variations are usually larger in the *B* band than in the *R* band, sometimes those amplitudes of variation were comparable.

5.4 Spectral variations

In Fig. 6 we have plotted the spectral indices α in the optical band against synchrotron peak frequency ($\nu_{\rm peak}$) for all classes of blazars. The values of α have been taken from our new measurements of these sources and have been supplemented by data for some more sources from Fiorucci et al. (2004) and Hu et al. (2006). Synchrotron peak frequencies of these sources have been taken from Nieppola et al. (2006) and Planck Collaboration et al. (2011). Spectral variations of these classes of blazars are discussed below.

5.4.1 LSPs

5.4.1.1 BL Lacs. For LSPs, we expect optical spectral indices $\alpha_{\rm ave} > 1$ due to their being on the descending part of the first bump of the SED. In this part of the spectrum we expect the spectral index to have broken so that $\alpha \approx \alpha_{\rm thin} + 1/2$, where $\alpha_{\rm thin} \simeq 0.5$–$0.7$. We have 11 LSPs in this sample and indeed all save 1 have $\alpha_{\rm ave} > 1$. From Fig. 6, it is clear that the distribution of spectral indices in the optical clustered around 1.5. The average of the spectral slopes of these LSPs is ∼1.5 excluding the two anomalous sources PKS 2032+107 and AO 0235+164. Chiang & Böttcher (2002) demonstrate that for a broad range of particle injection distributions, synchrotron self-Compton (SSC) loss dominated synchrotron emission exhibits exactly this kind of spectral slope. Hence, SSC models fit the optical emission for LSPs very well.

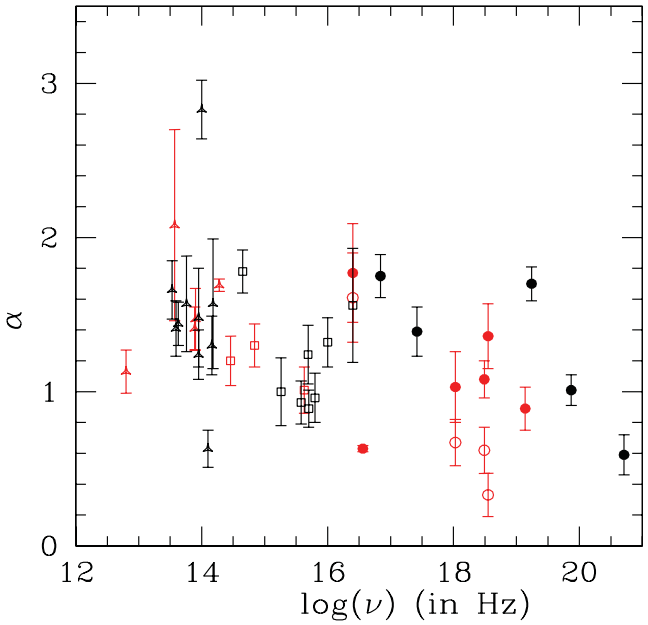

Figure 6. Spectral indices, α, against $\log(\nu_{\rm peak})$ for LSPs, ISPs and HSPs. Red symbols are αs calculated from our data and black symbols are αs taken from literature. Triangles represent LSPs, squares ISPs and filled circles HSPs. Open red circles represent the αs of four sources (1ES 2344+514, Mrk 421, 1ES 1959+650 and 1ES 1426+428, from left to right) after host galaxy subtraction.

5.4.1.2 FSRQs. Since FSRQs are a subclass of LSPs, we expect the optical spectral index also should be greater than 1. However, FSRQs show strong emission lines and a thermal contribution that may be comparable to the synchrotron emission in the optical spectral region. The optical emission of FSRQs is often strongly contaminated by thermal emission from the accretion disc and it is shown by the presence of the 'big blue bump' in the optical/UV region. This contribution was clearly shown in the SED of 3C 273 by Türler et al. (1999) and the mean optical spectral slope was calculated to be 0.6 by Fiorucci et al. (2004). However, for other two sources, 3C 454.3 and 3C 279, the spectral slopes are 1.47 and 1.13, respectively. That indicates the optical spectra of 3C 454.3 is likely dominated by the synchrotron component. This interpretation is supported by the facts that 3C 454.3 strong variability in our observations and was in very high state (Gaur et al. 2012a). But 3C 279 seems to be in intermediate state during our observations and thermal component is also playing role with synchrotron component.

5.4.2 ISPs

For the BL Lacs showing intermediate behaviour, we expect the $\alpha_{\rm ave} \geq 1$. We have 11 ISP sources, and the average of their spectral indices is 1.19. This supports the hypothesis that synchrotron emission dominates the optical band of these sources too.

5.4.3 HSPs

The spectral slopes of the HSPs scatters in the range between 0.5 and 1.8, while the predicted spectral slope under simple pure

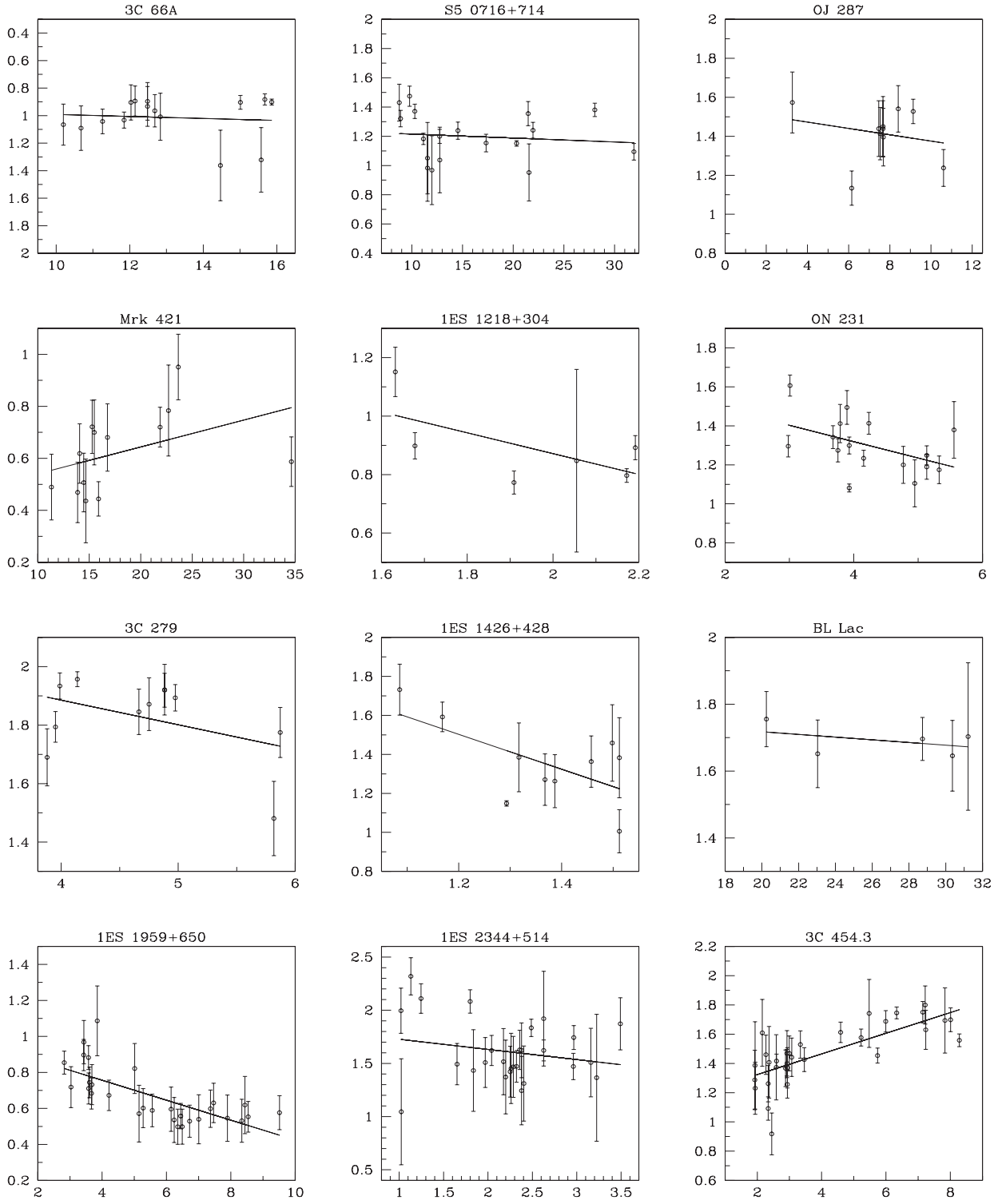

Figure 7. Dependence of the spectral slope on intensity for blazars. *X*-axis is spectral slope and *Y*-axis is flux in *R* band (mJy).

synchrotron emission models should be less than or equal to 0.75 or 0.80, corresponding to the spectral index of optically thin synchrotron-emitting plasma, $\alpha_{\rm thin}$ (Urry & Padovani 1995). This indicates that the optical emission of HSPs is contaminated by other components, such as a thermal contribution from the accretion disc or host galaxy, or else includes significant amounts of non-thermal emission originating from different regions of the relativistic jets. Furthermore, HSPs are more generally stable in the optical bands, while great flares and SED changes are frequently seen to be confined to the X- and γ-rays. This is consistent with the optical emission coming from a different region of the jet or with it being strongly diluted by thermal emission from the galaxy. For the nearby blazars, the host galaxy contribution is probably important (Pian et al. 1994). For Mrk 421, Tosti et al. (1998a)

determined the spectral slope to be $\alpha = 0.85$ after the subtraction of an estimated host galaxy contribution. We determined the spectral indices of six HSPs and for three of them α could be found with the host galaxy contribution included as well as after the host galaxy subtraction (Table 7). For Mrk 421, α is found to be 1.08 and 0.619 before and after the host galaxy contribution, respectively, and for 1ES 1959+650, α is found to be 1.03 and 0.67 before and after the host galaxy contribution is removed, respectively. Here we can say that there certainly is large deformation of the optical spectra of these HSPs due to the thermal contribution from the host galaxies. However, for 1ES 2344+514, α is not affected much, with high values of 1.77 and 1.61 before and after the galaxy subtraction. So for this source, the optical emission may only be contaminated by non-thermal emission originating from elsewhere in the relativistic jet.

5.4.4 Spectral slope variability

We have investigated the possible correlations between the source intensity and the slope of the optical SED. Fig. 7 shows the variability relations between the spectral slopes and the *R*-band fluxes (in mJy) for 12 blazars. A linear regression analysis was applied to each blazar and the linear regression slopes b, their standard deviations, corresponding correlation coefficients and their respective p values are listed in Table 7. Out of 15 sources studied, 1ES 0806+524, 1ES 1218+304, 1ES 1426+428, 1ES 1959+650, 3C 454.3 and 1ES 2344+514 showed rather significant correlations ($r > 0.6$) between the source intensity and spectral slopes. From the above sources, a tendency of spectral flattening when brightening has been seen for HSPs. This trend has been seen for both HSPs and LSPs by other investigators (e.g. Sikora et al. 2001; Spada et al. 2001; Chiang & Böttcher 2002; Vagnetti et al. 2003). However, the FSRQ 3C 454.3 has a tendency to show a spectrum that becomes steeper when the object becomes brighter, which has also been seen by previous authors (Miller 1981; Ramírez et al. 2004). On the other hand, the FSRQ 3C 279 has shown the opposite tendency but it is quite weak, having $r = 0.42$. For the other three LSPs (3C 66A, S5 0716+714 and OJ 287), we found no significant correlation between flux and spectral slope. For J0211+1051, ON 231 and BL Lac, we found negative correlations between spectral slope and *R*-band flux ($r > 0.40$) but they are not significant at a 0.95 confidence level. Only Mrk 421 showed a positive correlation between α and R magnitudes, but it is very weak, having $r = 0.4$.

6 CONCLUSIONS

We have carried out multiband optical photometry of a sample of 11 blazars including four HSPs, four LSPs and three ISPs during 2009–2011 on short-term time-scales. We found significant flux variations in all the sources except for 1ES 1218+304 and 1ES 1553+113 on short-term time-scales. Furthermore, we searched for colour variations in the sources; only three sources (AO 0235+164, S5 0716+714 and 1ES 1426+428) showed significant colour variations on short-term time-scales. We have studied IDV for four sources (S5 0716+714, OJ 287, 1ES 1426+428 and 1ES 1553+113) during 18 nights and found genuine IDV in 6 nights. We examined blazar colours for IDV and found significant ($B - R$) colour variations on only 2 nights.

We searched for possible correlations between colour and magnitude and found that six out of 10 BL Lacs followed the bluer-when-brighter trend; however, five sources (four BL Lacs and one FSRQ) lacked any such correlations. We studied the optical spectra of a total of 15 sources (including six HSPs, six LSPs and three ISPs) and compared these subclasses of blazars to provide some useful information on the emission components and emission mechanisms. LSP objects are extremely variable in optical bands and the average of the spectral slope of LSPs $\alpha \sim 1.5$, is in agreement with the SSC model. However, the SED of FSRQs probably has a contribution from a thermal bump that can noticeably contaminate the synchrotron component. The HSP spectral index varied from 0.5 to 1.8, which indicate that in addition to the synchrotron emission they have contributions by components such as quasi-thermal emission from the accretion disc or non-thermal emission originating from different regions in the jet. For some HSPs, the thermal contribution of the host galaxy plays an important role. This is clearly seen in Table 7 where we have been able to correct the spectral index for the host galaxy contribution for some nearby HSPs for which the galaxy could be resolved. The optical spectra of some of the sources become flatter when they brighten; however, for some sources we found no correlations or very weak opposite correlations. The relation between spectral slope and R magnitude of FSRQs suggests that the emission of FSRQs probably contains a thermal bump contribution and that this thermal component must be incorporated in detailed studies of individual sources.

ACKNOWLEDGMENTS

We thank the referee Dr E. Valtaoja for constructive comments that have helped us to improve the paper. We are thankful to Dr K. Nilsson for discussion about host galaxy contributions to observed flux. This research was partially supported by Scientific Research Fund of the Bulgarian Ministry of Education and Sciences (BIn – 13/09 and DO 02-85) and by Indo-Bulgaria bilateral scientific exchange project INT/Bulgaria/B-5/08 funded by DST, India. The Skinakas Observatory is a collaborative project of the University of Crete, the Foundation for Research and Technology – Hellas, and the Max-Planck-Institut für Extraterrestrische Physik.

REFERENCES

Abdo A. A. et al., 2009, ApJ, 707, 1310
Abdo A. A. et al., 2010, ApJ, 716, 30
Abraham Z., 2000, A&A, 355, 915
Acciari V. A. et al., 2008, ApJ, 684, L73
Acciari V. A. et al., 2010, ApJ, 709, L163
Aharonian F. et al., 2005, A&A, 437, 95
Aharonian F. et al., 2006, A&A, 448, L43
Albert J. et al., 2006, ApJ, 642, 119
Albert J. et al., 2007, ApJ, 654, L119
Bauer A., Baltay C., Coppi P., Ellman N., Jerke J., Rabinowitz D., Scalzo R., 2009, ApJ, 699, 1732
Biermann P. et al., 1981, ApJ, 247, L53
Biraud F., 1971, Nat, 232, 178
Böttcher M. et al., 2003, ApJ, 596, 847
Böttcher M. et al., 2007, ApJ, 670, 968
Böttcher M. et al., 2009, ApJ, 694, 174
Bramel D. A. et al., 2005, ApJ, 629, 108
Brown L. M. J., Robson E. I., Gear W. K., Smith M. G., 1989, ApJ, 340, 150
Browne I. W. A., 1971, Nat, 231, 515
Carini M. T., Miller H. R., 1992, ApJ, 385, 146
Chiang J., Böttcher M., 2002, ApJ, 564, 92
Costamante L. et al., 2001, A&A, 371, 512
de Diego J. A., 2010, AJ, 139, 1269
Donato D., Sambruna R. M., Gliozzi M., 2005, A&A, 433, 1163

Edelson R. A., Krolik J. H., 1988, ApJ, 333, 646
Emmanoulopoulos D., McHardy I. M., Uttley P., 2010, MNRAS, 404, 931
Falomo R., Treves A., 1990, PASP, 102, 1120
Falomo R., Scarpa R., Bersanelli M., 1994, ApJS, 93, 125
Fan J. H., Lin R. G., 1999, ApJS, 121, 131
Fan J. H., Lin R. G., 2000, ApJ, 537, 101
Fan J. H. et al., 1998, A&AS, 133, 163
Fan J. H., Zhang Y. W., Qian B. C., Tao J., Liu Y., Hua T. X., 2009, ApJS, 181, 466
Ferrero E., Wagner S. J., Emmanoulopoulos D., Ostorero L., 2006, A&A, 457, 133
Fiorucci M., Ciprini S., Tosti G., 2004, A&A, 419, 25
Foschini L. et al., 2006, A&A, 455, 871
Fossati G., Maraschi L., Celotti A., Comastri A., Ghisellini G., 1998, MNRAS, 299, 433
Fossati G. et al., 2008, ApJ, 677, 906
Fukugita M., Shimasaku K., Ichikawa T., 1995, PASP, 107, 945
Gaur H., Gupta A. C., Lachowicz P., Wiita P. J., 2010, ApJ, 718, 279
Gaur H., Gupta A. C., Wiita P. J., 2012a, AJ, 143, 23
Gaur H. et al., 2012b, MNRAS, 420, 3147
Gear W. K., Robson E. I., Brown L. M. J., 1986, Nat, 324, 546
Ghisellini G. et al., 1997, A&A, 327, 61
Ghosh K. K., Ramsey B. D., Sadun A. C., Soundararajaperumal S., 2000, ApJS, 127, 11
Giommi P., Ansari S. G., Micol A., 1995, A&AS, 109, 267
Gopal-Krishna, Subramanian K., 1991, Nat, 349, 766
Green R. F., Schmidt M., Liebert J., 1986, ApJS, 61, 305
Gu M. F., Lee C.-U., Pak S., Yim H. S., Fletcher A. B., 2006, A&A, 450, 39
Gupta A. C., Fan J. H., Bai J. M., Wagner S. J., 2008, AJ, 135, 1384
Gupta A. C., Srivastava A. K., Wiita P. J., 2009, ApJ, 690, 216
Hartman R. C. et al., 1996, ApJ, 461, 698
Hartman R. C. et al., 1999, ApJS, 123, 79
Hawkins M. R. S., 2002, MNRAS, 329, 76
Heidt J., Wagner S. J., 1996, A&A, 305, 42
Horan D. et al., 2002, ApJ, 571, 753
Hovatta T., Tornikoski M., Lainela M., Lehto H. J., Valtaoja E., Torniainen I., Aller M. F., Aller H. D., 2007, A&A, 469, 899
Hu S. M., Zhao G., Guo H. Y., Zhang X., Zheng Y. G., 2006, MNRAS, 371, 1243
Hufnagel B. R., Bregman J. N., 1992, ApJ, 386, 473
Jannuzi B. T., Smith P. S., Elston R., 1993, ApJS, 85, 265
Jannuzi B. T., Smith P. S., Elston R., 1994, ApJ, 428, 130
Katz J. I., 1997, ApJ, 478, 527
Kirk J. G., Rieger F. M., Mastichiadis A., 1998, A&A, 333, 452
Lanzetta K. M., Turnshek D. A., Sandoval J., 1993, ApJS, 84, 109
Lichti G. G. et al., 2008, A&A, 486, 721
Liu F. K., Liu B. F., Xie G. Z., 1997, A&AS, 123, 569
Maccagni D., Garilli B., Schild R., Tarenghi M., 1987, A&A, 178, 21
Madejski G. M., Sikora M., Jaffe T., Błażejowski M., Jahoda K., Moderski R., 1999, ApJ, 521, 145
Maesano M., Montagni F., Massaro E., Nesci R., 1997, A&AS, 122, 267
Maraschi L. et al., 1994, ApJ, 435, L91
Marcha M. J. M., Browne I. W. A., Impey C. D., Smith P. S., 1996, MNRAS, 281, 425
Marscher A. P., 1996, in Miller H. R., Webb J. R., Noble J. C., eds, ASP Conf. Ser. Vol. 110, Blazar Continuum Variability. Astron. Soc. Pac., San Francisco, p. 248
Marscher A. P., Gear W. K., 1985, ApJ, 298, 114
Marscher A. P. et al., 2008, Nat, 452, 966
Massaro E., Nesci R., Maesano M., Montagni F., D'Alessio F., 1998, MNRAS, 299, 47
Massaro F., Giommi P., Tosti G., Cassetti A., Nesci R., Perri M., Burrows D., Gerehls N., 2008, A&A, 489, 1047
Mastichiadis A., Kirk J. G., 2002, Publ. Astron. Soc. Australia, 19, 138
Miller H. R., 1975, ApJ, 201, L109
Miller H. R., 1981, ApJ, 244, 426
Miller H. R., Green R. F., 1983, BAAS, 15, 957
Miller J. S., French H. B., Hawley S. A., 1978, in Wolfe A. M., ed., Pittsburgh Conf. BL Lac Objects. Univ. of Pittsburgh, Pittsburgh, p. 176
Miller H. R., Carini M. T., Gaston B. J., Hutter D. J., 1988, ESA SP-281, The Ultraviolet/Optical Variability of PG 1553+11. ESA, Noordwijk, p. 303
Montagni F., Maselli A., Massaro E., Nesci R., Sclavi S., Maesano M., 2006, A&A, 451, 435
Nieppola E., Tornikoski M., Valtaoja E., 2006, A&A, 445, 441
Nilsson K., Charles P. A., Pursimo T., Takalo L. O., Sillanpaeae A., Teerikorpi P., 1996, A&A, 314, 754
Nilsson K., Pasanen M., Takalo L. O., Lindfors E., Berdyugin A., Ciprini S., Pforr J., 2007, A&A, 475, 199
Nilsson K., Pursimo T., Sillanpää A., Takalo L. O., Lindfors E., 2008, A&A, 487, L29
Osterman M. A. et al., 2006, AJ, 132, 873
Ostorero L. et al., 2006, A&A, 451, 797
Padovani P., Giommi P., 1996, MNRAS, 279, 526
Padovani P., Costamante L., Giommi P., Ghisellini G., Celotti A., Wolter A., 2004, MNRAS, 347, 1282
Perri M. et al., 2003, A&A, 407, 453
Petry D. et al., 2000, ApJ, 536, 742
Pian E., Falomo R., Scarpa R., Treves A., 1994, ApJ, 432, 547
Planck Collaboration et al., 2011, A&A, 536, A15
Punch M. et al., 1992, Nat, 358, 477
Pursimo T. et al., 2000, A&AS, 146, 141
Raiteri C. M. et al., 2001, A&A, 377, 396
Raiteri C. M. et al., 2003, A&A, 402, 151
Raiteri C. M. et al., 2005, A&A, 438, 39
Raiteri C. M., Villata M., Kadler M., Krichbaum T. P., Böttcher M., Fuhrmann L., Orio M., 2006a, A&A, 452, 845
Raiteri C. M. et al., 2006b, A&A, 459, 731
Raiteri C. M. et al., 2009, A&A, 507, 769
Ramírez A., de Diego J. A., Dultzin-Hacyan D., González-Pérez J. N., 2004, A&A, 421, 83
Rani B. et al., 2010a, MNRAS, 404, 1992
Rani B., Gupta A. C., Joshi U. C., Ganesh S., Wiita P. J., 2010b, ApJ, 719, L153
Ravasio M., Tagliaferri G., Ghisellini G., Tavecchio F., Böttcher M., Sikora M., 2003, A&A, 408, 479
Rebillot P. F. et al., 2006, ApJ, 641, 740
Rector T. A., Gabuzda D. C., Stocke J. T., 2003, AJ, 125, 1060
Remillard R. A., Tuohy I. R., Brissenden R. J. V., Buckley D. A. H., Schwartz D. A., Feigelson E. D., Tapia S., 1989, ApJ, 345, 140
Romero G. E., Cellone S. A., Combi J. A., 1999, A&AS, 135, 477
Romero G. E., Cellone S. A., Combi J. A., 2000, A&A, 360, L47
Sambruna R. M., Maraschi L., Urry C. M., 1996, ApJ, 463, 444
Schlegel D. J., Finkbeiner D. P., Davis M., 1998, ApJ, 500, 525
Sikora M., Błażejowski M., Begelman M. C., Moderski R., 2001, ApJ, 554, 1
Sillanpää A., Haarala S., Valtonen M. J., Sundelius B., Byrd G. G., 1988, ApJ, 325, 628
Sillanpää A. et al., 1996a, A&A, 305, L17
Sillanpää A. et al., 1996b, A&A, 315, L13
Sitko M. L., Junkkarinen V. T., 1985, PASP, 97, 1158
Smith A. G., Nair A. D., 1995, PASP, 107, 863
Spada M., Ghisellini G., Lazzati D., Celotti A., 2001, MNRAS, 325, 1559
Spinrad H., Smith H. E., 1975, ApJ, 201, 275
Stalin C. S., Gopal-Krishna, Sagar R., Wiita P. J., Mohan V., Pandey A. K., 2006, MNRAS, 366, 1337
Stein W. A., Odell S. L., Strittmatter P. A., 1976, ARA&A, 14, 173
Stetson P. B., 1987, PASP, 99, 191
Stetson P. B., 1992, J. R. Astron. Soc. Can., 86, 71
Stickel M., Fried J. W., Kuehr H., 1993, A&AS, 98, 393
Stocke J. T., Morris S. L., Gioia I. M., Maccacaro T., Schild R., Wolter A., Fleming T. A., Henry J. P., 1991, ApJS, 76, 813
Takahashi T. et al., 2000, ApJ, 542, L105
Takalo L. O., Sillanpaeae A., Nilsson K., 1994, A&AS, 107, 497
Takalo L. O. et al., 1996, A&AS, 120, 313

Tornikoski M., Valtaoja E., Terasranta H., Smith A. G., Nair A. D., Clements S. D., Leacock R. J., 1994, A&A, 289, 673
Tosti G. et al., 1998a, A&A, 339, 41
Tosti G. et al., 1998b, A&AS, 130, 109
Tosti G. et al., 2002, A&A, 395, 11
Trèvese D., Vagnetti F., 2002, ApJ, 564, 624
Türler M. et al., 1999, A&AS, 134, 89
Ulrich M.-H., Kinman T. D., Lynds C. R., Rieke G. H., Ekers R. D., 1975, ApJ, 198, 261
Urry C. M., Padovani P., 1995, PASP, 107, 803
Urry C. M., Scarpa R., O'Dowd M., Falomo R., Pesce J. E., Treves A., 2000, ApJ, 532, 816
Vagnetti F., Trèvese D., Nesci R., 2003, ApJ, 590, 123
Valtaoja E., Teräsranta H., Tornikoski M., Sillanpää A., Aller M. F., Aller H. D., Hughes P. A., 2000, ApJ, 531, 744
Valtonen M., Ciprini S., 2012, MmSAI, 83, 219
Valtonen M. J. et al., 2008, Nat, 452, 851
Villata M., Raiteri C. M., Sillanpaa A., Takalo L. O., 1998, MNRAS, 293, L13
Villata M., Raiteri C. M., Popescu M. D., Sobrito G., De Francesco G., Lanteri L., Ostorero L., 2000, A&AS, 144, 481
Villata M. et al., 2002, A&A, 390, 407
Villata M. et al., 2009, A&A, 501, 455
von Montigny C. et al., 1995, ApJ, 440, 525
Wagner S. J., Witzel A., 1995, ARA&A, 33, 163
Wagner S., Sanchez-Pons F., Quirrenbach A., Witzel A., 1990, A&A, 235, L1
Wagner S. J. et al., 1996, AJ, 111, 2187
Webb J. R., Carini M. T., Clements S., Fajardo S., Gombola P. P., Leacock R. J., Sadun A. C., Smith A. G., 1990, AJ, 100, 1452
Webb J. R., Howard E., Benítez E., Balonek T., McGrath E., Shrader C., Robson I., Jenkins P., 2000, AJ, 120, 41
Wehrle A. E. et al., 1998, ApJ, 497, 178
Weistrop D., Shaffer D. B., Hintzen P., Romanishin W., 1985, ApJ, 292, 614
Wood K. S. et al., 1984, ApJS, 56, 507
Xie G. Z., Li K. H., Liu F. K., Lu R. W., Wu J. X., Fan J. H., Zhu Y. Y., Cheng F. Z., 1992, ApJS, 80, 683
Xie G. Z., Li K. H., Zhang X., Bai J. M., Liu W. W., 1999, ApJ, 522, 846

This paper has been typeset from a TEX/LATEX file prepared by the author.